

University of New Hampshire  
**University of New Hampshire Scholars' Repository**

---

Molecular, Cellular and Biomedical Sciences  
Scholarship

Molecular, Cellular and Biomedical Sciences

---

Winter 12-22-2017

# Comparative study of spinning field development in two species of araneophagic spiders (Araneae, Mimetidae, Australomimetes)

Mark A. Townley

*University of New Hampshire*, [mark.townley@unh.edu](mailto:mark.townley@unh.edu)

Danilo Harms

*University of Hamburg*

Follow this and additional works at: [https://scholars.unh.edu/mcbs\\_facpub](https://scholars.unh.edu/mcbs_facpub)

Part of the [Developmental Biology Commons](#), [Evolution Commons](#), and the [Zoology Commons](#)

---

## Recommended Citation

Townley, Mark A. and Harms, Danilo, "Comparative study of spinning field development in two species of araneophagic spiders (Araneae, Mimetidae, Australomimetes)" (2017). *Evolutionary Systematics*. 224.  
[https://scholars.unh.edu/mcbs\\_facpub/224](https://scholars.unh.edu/mcbs_facpub/224)

This Article is brought to you for free and open access by the Molecular, Cellular and Biomedical Sciences at University of New Hampshire Scholars' Repository. It has been accepted for inclusion in Molecular, Cellular and Biomedical Sciences Scholarship by an authorized administrator of University of New Hampshire Scholars' Repository. For more information, please contact [nicole.hentz@unh.edu](mailto:nicole.hentz@unh.edu).

# Comparative study of spinning field development in two species of araneophagic spiders (Araneae, Mimetidae, *Australomimetus*)

Mark A. Townley<sup>1</sup>, Danilo Harms<sup>2</sup>

<sup>1</sup> University Instrumentation Center, University of New Hampshire, 46 College Road, Durham, NH 03824, USA

<sup>2</sup> Zoological Museum, Center of Natural History, University of Hamburg, Martin-Luther-King-Platz 3, 20146 Hamburg, Germany

<http://zoobank.org/14A3FB08-01CC-47B6-A514-F314C2D7ABB4>

Corresponding author: Mark A. Townley (mark.townley@unh.edu)

## Abstract

Received 29 June 2017  
Accepted 2 September 2017  
Published 22 December 2017

Academic editor:  
Martin Husemann

## Key Words

Pirate spider  
Mimetidae  
*Australomimetus*  
spinneret  
spinning field  
molting  
silk gland  
tartipore

External studies of spider spinning fields allow us to make inferences about internal silk gland biology, including what happens to silk glands when the spider molts. Such studies often focus on adults, but juveniles can provide additional insight on spinning apparatus development and character polarity. Here we document and describe spinning fields at all stadia in two species of pirate spider (Mimetidae: *Australomimetus spinosus*, *A. djuka*). Pirate spiders nest within the ecribellate orb-building spiders (Araneoidea), but are vagrant, araneophagic members that do not build prey-capture webs. Correspondingly, they lack aggregate and flagelliform silk glands (AG, FL), specialized for forming prey-capture lines in araneoid orb webs. However, occasional possible vestiges of an AG or FL spigot, as observed in one juvenile *A. spinosus* specimen, are consistent with secondary loss of AG and FL. By comparing spigots from one stadium to tartipores from the next stadium, silk glands can be divided into those that are tartipore-accommodated (T-A), and thus functional during proecdysis, and those that are not (non-T-A). Though evidence was more extensive in *A. spinosus*, it was likely true for both species that the number of non-T-A piriform silk glands (PI) was constant (two pairs) through all stadia, while numbers of T-A PI rose incrementally. The two species differed in that *A. spinosus* had T-A minor ampullate and aciniform silk glands (MiA, AC) that were absent in *A. djuka*. First instars of *A. djuka*, however, appeared to retain vestiges of T-A MiA spigots, consistent with a plesiomorphic state in which T-A MiA (called secondary MiA) are present. T-A AC have not previously been observed in *Australomimetus* and the arrangement of their spigots on posterior lateral spinnerets was unlike that seen thus far in other mimetid genera. Though new AC and T-A PI apparently form throughout much of a spider's ontogeny, recurring spigot/tartipore arrangements indicated that AC and PI, after functioning during one stadium, were used again in each subsequent stadium (if non-T-A) or in alternate subsequent stadia (if T-A). In *A. spinosus*, sexual and geographic dimorphisms involving AC were noted. Cylindrical silk gland (CY) spigots were observed in mid-to-late juvenile, as well as adult, females of both species. Their use in juveniles, however, should not be assumed and only adult CY spigots had wide openings typical of mimetids. Neither species exhibited two pairs of modified PI spigots present in some adult male mimetids.

## Introduction

A common name applied to the family Mimetidae, pirate spiders, reflects their routine practice of invading the webs of other spiders and killing the occupant. Indeed,

web-building spiders, including spider eggs (Jackson and Whitehouse 1986, Jackson 1992), make up the bulk of the mimetid diet (Pekár et al. 2012). Moreover, mimetids can be described as true spider specialists (sensu Jackson and Cross 2015) given morphological, behavior-

al, and possibly biochemical (e.g., venom composition) adaptations towards araneophagy. For example, included in the behavioral repertoire of at least some mimetids is a vibratory aggressive mimicry that acts as a lure for prey spiders by simulating their insect prey (Jackson and Whitehouse 1986, Jackson 1992), potential mates (Czajka 1963, Kloock 2012), or more generalist web-invading spiders, con- or heterospecific (CT Kloock in Cormier 2017). Such adaptations do not, however, mean that mimetids are necessarily limited to feeding on spiders. Some, though not all (Bristowe 1941, Harms and Harvey 2009b), are reported to also feed on insects, by direct predation and kleptoparasitism (Cutler 1972, Jackson and Whitehouse 1986, Jackson 1992, Kloock 2001). The latter, kleptoparasitism or stealing booty (prey), not only fits the pirate moniker, but suggests a possible feeding-mode stepping stone on the evolutionary path to araneophagy (Shear 1981).

Several recent cladistic analyses, based partly or solely on sequence data, agree in placing Mimetidae within Araneoidea, and further agree that mimetids are closely related to the orb-web-building family Tetragnathidae (Blackledge et al. 2009, Dimitrov and Hormiga 2011, Dimitrov et al. 2012, Bond et al. 2014, Hormiga and Griswold 2014, Benavides et al. 2016, Dimitrov et al. 2016, Garrison et al. 2016, Wheeler et al. 2016). The possibility of a close relationship between these two families was raised earlier by Shear (1981) and Schütt (2000) based on morphological similarities and indicates that araneophagy, combined with a loss of web-building capacity, is a derived state in this family.

The family Mimetidae currently comprises some 150 species in 12 genera (World Spider Catalog 2017). Relationships were recently investigated using molecular data and there is now a modern phylogenetic framework for the family, albeit not including all recognized genera, from which to evaluate states of character evolution (Benavides et al. 2016). Within the family, the three genera *Mimetus*, *Ero*, and *Australomimetus* contain the bulk of species, although the generic concepts are in flux and at least *Mimetus* is clearly polyphyletic whilst the Australasian endemic *Australomimetus* is monophyletic (Harms and Dunlop 2009, Benavides et al. 2016). Mimetids occur on all continents except Antarctica, but *Australomimetus*, to which our two study species belong, is restricted to southeast Asia and Australasia (Harms and Harvey 2009a, b, Benavides et al. 2016) and may have diversified after the opening of the Tasman sea during the Gondwana break-up (Benavides et al. 2016).

Spinning fields on spider spinnerets contain the spigots through which silk gland products pass to the external environment. They provide a window to the silk glands, indicating the variety of silk gland types contained within the opisthosoma and their numbers. In mimetids, spigots of major ampullate, piriform, minor ampullate, aciniform, and cylindrical (= tubuliform) silk glands (MaA, PI, MiA, AC, CY, respectively) occupy the spinning fields. The roles of different silk glands have not been studied exten-

sively in this family, but if observations from other araneoids apply, then attachment disks and junctional cements are formed from PI secretions while draglines, bridging lines, prey-swathing fibers, and egg sacs contain MaA silk, MiA silk, AC silk, and CY silk, respectively, and each of these constructions may be supplemented, variably or consistently, by fibers from other silk gland types (Tillinghast and Townley 1994, Blackledge et al. 2011). Other structures in spinning fields, tartipores and nubbins [see Abbreviations and terminology ('Terminology'), Table 1], supply additional information about changes silk glands undergo in relation to the molt-intermolt cycle, evolutionary changes that have occurred in the spinning apparatus, and the ontogenetic fates of individual silk glands. The data obtained from spinning fields are most complete and observations most reliably interpreted when juvenile as well as adult specimens are examined, and especially when two or more sets of spinnerets from consecutive stadia are obtained from the same individual (Townley and Tillinghast 2009, Dolejš et al. 2014). Such observations are of value both intrinsically and for the many characters they provide for improving spider phylogenetic hypotheses.

In earlier studies, spinnerets from five species of *Australomimetus* were examined by scanning electron microscopy (SEM), all adults (Harms and Harvey 2009b, Townley and Tillinghast 2009, Townley et al. 2013). Here, we had the opportunity to examine and document spinnerets at all stadia in two species not previously examined, *Australomimetus spinosus* Heimer, 1986 and *A. djuka* Harms & Harvey, 2009b. These species are ecologically divergent, with *A. djuka* restricted to wet eucalypt forest and caves in far southwestern Australia and *A. spinosus* inhabiting rocky outcrops in drier areas of Western Australia. They also belong to different species-groups (Harms and Harvey 2009b) and these distinctions may be significant. As detailed below, *A. spinosus* possess a character state, the presence of tartipore-accommodated (T-A) [see Abbreviations and terminology ('Terminology'), Table 1] aciniform silk glands (AC) associated with the posterior lateral spinnerets (PLS), that has not previously been seen in any *Australomimetus* species and is also not present in *A. djuka*. Moreover, the spigots of these T-A AC have an arrangement on the PLS unlike that seen in other mimetid genera with PLS-associated T-A AC.

## Abbreviations and terminology

### Spinning apparatus abbreviations

1°	primary
2°	secondary
AC	aciniform silk gland
AG	aggregate silk gland
ALS	anterior lateral spinneret
Col	colulus
CY	cylindrical (= tubuliform) silk gland
FL	flagelliform silk gland

**Table 1.** Terminology used in this paper.

Term	Definition
Proecdysis	The period between apolysis (detachment of epidermis from old exoskeleton in preparation for deposition of new exoskeleton) and ecdysis (shedding of old exoskeleton)
Tartipore	A minute opening that forms during proecdysis within the developing new exoskeleton around a silk gland duct. It allows the duct to remain connected to a spigot on the old exoskeleton so silk can be drawn from that spigot throughout proecdysis. After ecdysis, the tartipore is non-functional but remains apparent in the exoskeleton.
Tartipore-accommodated (T-A) silk gland	A silk gland with a duct that remains connected to a spigot on the old exoskeleton throughout proecdysis because an opening (tartipore) forms in the developing new exoskeleton to accommodate the duct. This allows silk to be drawn from the silk gland throughout proecdysis. At ecdysis, the silk gland's spigot is cast off along with the rest of the old exoskeleton and its duct will not connect to a new spigot until a new exoskeleton forms during the following proecdysis. Thus, these silk glands function in alternate stadia.
Non-tartipore-accommodated (Non-T-A) silk gland	A silk gland from which silk cannot be drawn during proecdysis because its duct becomes detached from its spigot around apolysis. The duct can, however, then attach to a spigot on the developing new exoskeleton, allowing these silk glands to function in consecutive stadia.
Primary (1°) ampullate silk glands	Larger ampullate silk glands that are non-T-A. They include 1° major ampullate and 1° minor ampullate silk glands (1° MaA, 1° MiA).
Secondary (2°) ampullate silk glands	Smaller ampullate silk glands that are T-A. They include 2° major ampullate and 2° minor ampullate silk glands (2° MaA, 2° MiA).
Nubbin	A vestigial spigot. Three types are recognized: 1) ontogenetic: forms at a site occupied by a functional spigot during an earlier stadium; 2) phylogenetic: forms at a site occupied by a functional spigot in an ancestor; 3) teratological: forms seemingly at random, usually asymmetrically (on one spinneret but not its pair), as a result of a developmental anomaly.

MaA	major ampullate silk gland
MiA	minor ampullate silk gland
MoPI	modified piriform silk gland
PI	piriform silk gland
PLS	posterior lateral spinneret
PMS	posterior median spinneret
T-A	tartipore-accommodated

### Terminology

Located in the spinning fields of some spinnerets, **tartipores** form and function only during **proecdysis** (Table 1), acting within the underlying new exoskeleton as short conduits for those silk gland ducts that remain connected to spigots on the overlying old exoskeleton. An example of a tartipore that was preserved while functioning during proecdysis is shown in Fig. 4C.

Murphy and Roberts (2015) substituted the term ‘cicatix’ for ‘tartipore’ on the grounds that “...tartipores... is misleading since they are not, in any sense, pores.” It is true that after ecdysis, after tartipores have served their purpose, they no longer function as pores, but during proecdysis they can be described as pores, if we accept ‘pore’ to be a minute opening in a surface. It would be disingenuous, however, not to acknowledge that the term ‘tartipore’ was initially applied, not to proecdysial tartipores functioning as pores, but to post-ecdysial, post-functional tartipores (Shear et al. 1989, Yu and Coddington 1990). Townley and Tillinghast (2003) continued this restricted, post-ecdysial use of the term and thus defined tartipores as cuticular scars, very much in accord with Murphy and Roberts’ (2015) use of ‘cicatixes’. The proecdysial, functional form of tartipores were referred to as ‘tartipore progenitors’. Put another way (with the objection of Murphy and Roberts in mind), these structures were recognized as definitive tartipores only once they no longer functioned as pores! In practice, maintaining a terminological distinction between proecdysial ‘tartipore progenitors’ and post-ecdy-

sial ‘tartipores’ was found to be unnecessary, more confusing than clarifying, and, thus, ‘tartipore progenitors’ were subsequently also referred to as ‘tartipores’ (Townley and Tillinghast 2009). We concur that a single term should be applied to these conduits, whether functional or post-functional, and since they are not scars during proecdysis, nor pores after ecdysis, it can be argued that neither ‘cicatix’ nor ‘tartipore’ is entirely fitting. But as ‘tartipore’ is already well-established, we will continue to use it.

Only the ducts of some silk glands remain connected to the old exoskeleton during proecdysis and result in tartipores forming in the developing exoskeleton around the ducts. These silk glands are said to be **tartipore-accommodated (T-A)** and can have silk drawn from them during proecdysis. The ducts of **non-tartipore-accommodated (non-T-A)** silk glands lose their connection to the old exoskeleton around apolysis, do not give rise to tartipores, and therefore the spider cannot draw silk from them during proecdysis. In some spider clades, such as the ecribellate haplogyne Synspermiata (Platnick et al. 1991, Michalik and Ramírez 2014, Garrison et al. 2016, Wheeler et al. 2016), all silk glands are non-T-A. The two *Australomimetes* species examined in this study have both T-A and non-T-A versions of major ampullate, minor ampullate, and piriform silk glands (MaA, MiA, PI). *A. spinosus* also has T-A and non-T-A aciniform silk glands (AC), whereas *A. djuka* only has non-T-A AC, and the female-specific cylindrical silk glands (CY) are exclusively non-T-A in both species. Those MaA and MiA that are non-T-A are called **primary (1°) MaA/MiA** while those that are T-A are called **secondary (2°) MaA/MiA**. This nomenclature reflects both the larger size of the 1° MaA/MiA and their use over a greater portion of juvenile stadia: from each ecdysis to the next apolysis, as opposed to the 2° MaA/MiA that appear to function, at least in *Araneus*, only very shortly before and during proecdysis (Townley et al. 1993, Tillinghast and Townley 1994). Typical of araneoids, in *Australomimetes*, 1° MaA/MiA function

in juveniles and adults while 2° MaA/MiA function only in juveniles (and some *Australomimetes* species, like *A. djuka*, lack functional 2° MiA entirely).

Depending on species, sex, spinneret, instar, and maturity, certain spinning fields consistently contain vestigial spigots, termed **nubbins**, at sites occupied by functional spigots either in earlier instars (**ontogenetic nubbins**; often present in adults, such as 2° MaA/MiA nubbins) or in ancestors (**phylogenetic nubbins**). Examples of both these types of nubbins were observed during this study and are noted below. In the literature up through about 1994 (and sometimes beyond), the structures now identified as 2° MaA/MiA tartipores were generally referred to as nubbins [non-vestigial-type nubbins in Townley et al. (1993)] because the terms ‘nubbin’ and ‘tartipore’ were originally applied to non-spigot protuberances in spinning fields on the basis of whether or not they can be individually specified (Coddington 1989, Yu and Coddington 1990). Later, once the very different developmental origins of nubbins and tartipores were better understood, ‘nubbin’ was restricted to its current meaning of vestigial spigot (Townley 1993, Townley and Tillinghast 2003). The above terms are summarized in Table 1.

With our focus on external features of the exoskeleton, we consider ecdysis to be the event that separates **instars** (the spiders themselves) and **stadia** (the periods of time between ecdyses or from ecdysis to death) since, from an external view, it is at ecdysis that there is a change of exoskeleton. Following apolysis, we apply the term **pharate instar** to only that portion of a proecdysial spider from the new exoskeleton inward. Thus, using the example of a specimen presented extensively in this paper, a 4<sup>th</sup> instar that undergoes apolysis, considered as a whole, remains a 4<sup>th</sup> instar throughout proecdysis, and the pharate 5<sup>th</sup> instar constitutes only a part (albeit the predominant part) of this proecdysial

4<sup>th</sup> instar. As proposed by Downes (1987), and adopted by others (e.g., Townley and Tillinghast 2009, Wolff and Hilbrant 2011, Hilbrant et al. 2012, Mittmann and Wolff 2012), when an embryo hatches, the **postembryo** is released, and ecdysis in the postembryo, including the discarding of its **exuvium** (shed exoskeleton), produces the **1<sup>st</sup> instar** and marks the start of the **1<sup>st</sup> stadium**. The molt between the postembryonic stage and 1<sup>st</sup> stadium is taken to be the **1<sup>st</sup> molt** (Downes 1987). Subsequent ecdyses produce consecutively numbered instars and stadia. Fig. 1 schematically summarizes these terms as used in this paper. Though some definitions of instar/stadium exclude adults (Carlson 1983), we distinguish spiders that molted 5 times before becoming adults from those that molted 6 times by referring to 5<sup>th</sup> stadium and 6<sup>th</sup> stadium adults, respectively.

## Materials and methods

### Collection details and rearing methods

Specimens of *Australomimetes spinosus* were reared in captivity from egg sacs collected at Yandin-Lookout, Western Australia (30°46'23"S, 115°36'31"E) in August 2014. *Australomimetes spinosus* is the only mimetid spider that occurs in the Yandin Nature Reserve which comprises open eucalypt woodland and *Xanthorrhoea* shrubland on rocky outcrops. All egg sacs, containing 10–25 eggs each, were collected from under large rocks and boulders together with females. In the lab, up to four egg sacs were placed in glass jars capped with nylon and the emerging spiderlings were fed with prey spiders (Theridiidae) collected in the field. To avoid cannibalism in *A. spinosus* post-molt, the spiderlings were progressively separated from the 3<sup>rd</sup> stadium onwards and 3–5 speci-

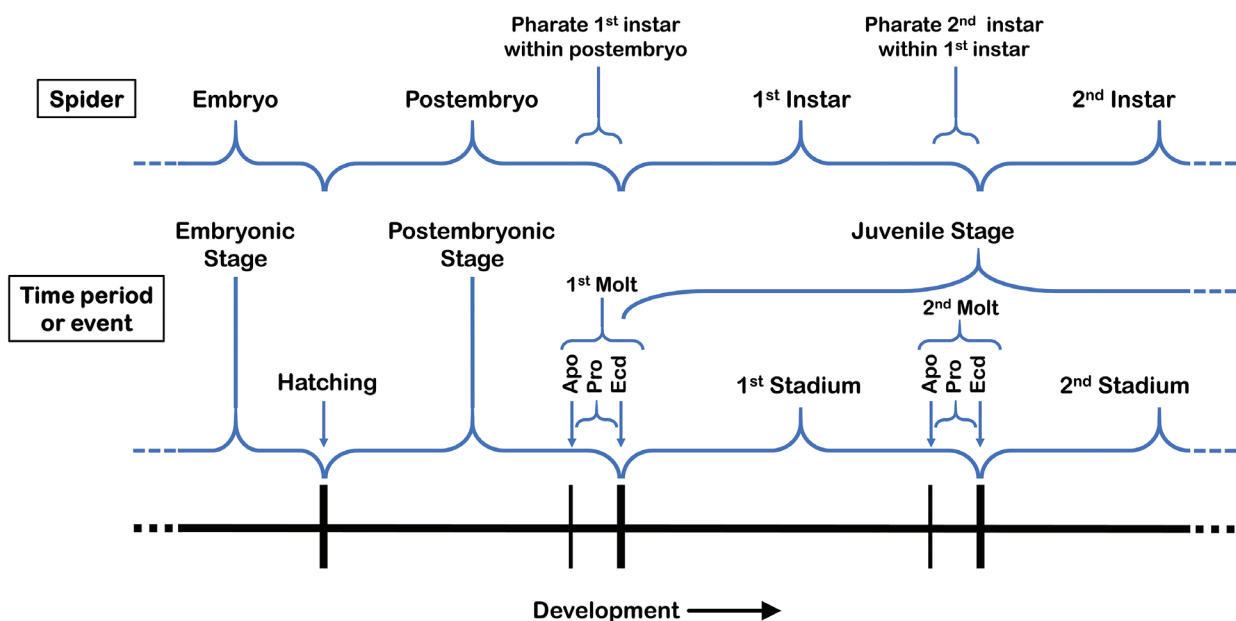


**Figure 1.** Developmental terms as applied in this paper, largely based on the proposal of Downes (1987). Indicated relative durations of stages are not intended to be accurate. Apo, apolysis; Ecd, ecdysis; Pro, proecdysis.

mens of later instars were reared in small jars with sufficient prey and some paper tissue. Specimens of all life stages were euthanized in 100% ethanol between August 2014 and January 2015, then stored in a freezer for further analyses. Exuvia of representative specimens were also preserved in ethanol post-molt. Additional museum specimens of *A. spinosus* were also available from Western Australia, Queensland, and New South Wales, collected between January 1992 and July 2014 and stored in 70–75% ethanol. All specimens of *A. djuka* were from the collections of the Western Australian Museum (WAM), and stored in 70–75% ethanol. This species has a larger body size but also considerably higher moisture requirements than *A. spinosus*. It is endemic to the southwest of Western Australia and has been collected from limestone caves in Yanchep National Park but also dense bark accumulations in undisturbed karri (*Eucalyptus diversicolor*) forest. Additional information on material examined is given in Suppl. material 1.

### Spinnerets examined

A total of 11 sets of spinnerets (6 spinnerets/set; 1 set/abdominal exoskeleton) from *A. djuka* and 63 sets of spinnerets from *A. spinosus* were examined by SEM (Table 2). These included one or more sets from each instar that has a functioning spinning apparatus (1<sup>st</sup> to 6<sup>th</sup> instars). Of the 63 *A. spinosus* sets, 49 were from 1<sup>st</sup> to 5<sup>th</sup> instars, all juveniles from Western Australia and laboratory-raised. The other 14 sets, which included those from all 9 *A. spinosus* adults that were examined, were from spiders field-collected either in Western Australia or in Queensland or New South Wales (Table 3). The 49 sets of spinnerets from laboratory-raised specimens included 7 from exuvia of 2<sup>nd</sup> instars and 7 from exuvia of 3<sup>rd</sup> instars. Later spinnerets from at least some of the spiders that shed these exuvia were also examined. In addition, one laboratory-raised 4<sup>th</sup> instar in proecdysis yielded two sets of spinnerets, one from the old exoskeleton, one from the new (pharate 5<sup>th</sup> instar's) exoskeleton. Thus, an unknown number of spiders, but probably  $\leq 37$ , gave rise to the 49 sets of spinnerets from laboratory-raised spiders. With the exception of the two sets from the proecdysial 4<sup>th</sup> instar, we do not know which sets of spinnerets came from the same individual. Overall, this is one of the more comprehensive spinneret data sets on juvenile spiders to date, covering all life stadia, 1<sup>st</sup> to adult, in these two species.

### Scanning electron microscopy (SEM) of spinnerets: preparation and examination

Intact sets of spinnerets, including underlying tissues and small amounts of surrounding exoskeleton, were cut off ethanol-preserved specimens of the two *Australomimetes* species using Vannas spring scissors (Fine Science Tools, 15000-08) while being viewed through an Olympus SZX12 stereo microscope. They were immersed in Novex® Tris-glycine sodium-dodecyl-sulfate (SDS) buffer (ThermoFisher Scientific, LC2675) at 2X-strength for

at least 3 days at 4°C. If underlying tissues did not show signs of partial solubilization in the buffer (expansion, increased translucence, separation from exoskeleton), incubation was continued at room temperature for up to 4 months. After a brief (5 min) rinse in commercial contact lens saline solution, spinnerets were further cleaned, and remaining underlying tissues digested, in Oxysept® Disinfecting Solution containing one Oxysept® Neutralizing Tablet and one Ultrazyme® Enzymatic Cleaner Tablet (all Abbott Medical Optics, intended for use with soft contact lenses) according to manufacturer's instructions. This treatment exposed spinnerets to 3% H<sub>2</sub>O<sub>2</sub> and subtilisin A and was allowed to proceed until underlying tissues were no longer visible, occasionally requiring overnight incubation. Spinnerets were then transferred to a Petri dish containing a wax layer overlaid with the above Novex® buffer. The tips of pins of various sizes projected 1–3 mm upward from the wax layer (Townley and Tillinghast 2009). Each spinneret in a set was pulled down onto a pin tip of appropriate diameter to expand the spinneret as fully as possible. As Fig. 9G demonstrates, expansion was not always entirely successful. Spinnerets were then dehydrated through an ethanol series (30%, 50%, 70%, 85%, 95%, 100%, 100%; at least 1 day in each), followed by transfer into microporous specimen capsules [11 x 12 mm, 78 µm pore size, 1 set of spinnerets/capsule; Electron Microscopy Sciences (EMS), 70187-10] that were submerged in fresh 100% ethanol. All transfers of spinnerets from one solution to another were accomplished using transfer pipets so that severed spinnerets were always in liquid from their initial immersion in Novex® buffer to their transfer to the microporous capsules. Capsules were placed in the ethanol-filled chamber of a Tousimis Samdri-795 critical point dryer and dried. Spinnerets were then affixed to aluminum SEM specimen pin mounts (EMS, 75160) using double-sided conductive carbon adhesive tabs (EMS, 77825-09) and PELCO® conductive carbon glue (Ted Pella Inc., 16050), sputter-coated with about 20 nm gold/palladium, and examined on a Tescan Lyra3 XMU field-emission SEM (6 kV, beam intensity 6).

Some 2<sup>nd</sup> and 3<sup>rd</sup> stadia spinnerets were obtained from exuvia that were initially stored in 70–75% ethanol, but were subsequently immersed in the aforementioned SDS-containing Novex® buffer for at least 2 months at 4°C. These were prepared like the above spinnerets from intact specimens except that they were not treated with the H<sub>2</sub>O<sub>2</sub>/subtilisin A solution and they were not intentionally separated from the rest of the exuvium, though separation often resulted nonetheless from the act of pulling the spinnerets down onto the tips of pins to expand them.

Diameters of AC spigot openings, presented in Figs 7E, G, 8E, 9J, K, and 10F, were obtained using the measurement tool in Tescan's Lyra 3 Control Software. Because borders of some openings deviated noticeably from a circle, each value given in a figure is the mean of two measurements: the opening's widest diameter and that perpendicular to the widest.

Table 2. Spigot, tartipore, and nubbin complements on spinnerets of *Australomimetes djuka* and *Australomimetes spinosus*.

Instar	Species	Sex	N <sup>b</sup>	ALS				PMS				PLS				
				1° MaA spigot	2° MaA spigot	2° MaA tartipore <sup>c</sup>	2° MaA nubbin	PI spigots	PI tartipores	1° MiA spigot	2° MiA tartipore <sup>c</sup>	2° MiA nubbin	AC spigots	AC tartipores	CY spigot	AC tartipores
1st	<i>Australomimetes djuka</i>	unknown	2	1	1	1 prim.	0	4	0	0	1	0	0	0	0	0
1st	<i>Australomimetes spinosus</i>	unknown	6	1	1	1 prim.	0	4	0	1	1	0	2	0	3	0
2nd	<i>Australomimetes djuka</i>	unknown	1	1	1	1	0	7.5 (7-8)	2	0	0	0	1	0	2	0
2nd	<i>Australomimetes spinosus</i>	unknown	13	1	1	1	0	8.2 ± 0.12 (7-10)	2	1	1	0	2	0	3.1 ± 0.08 (3-4)	0
3rd	<i>Australomimetes djuka</i>	unknown	1	1	1	1	0	12.0 (11-13)	4	1	0	0	2	0	3	0
3rd	<i>Australomimetes spinosus</i>	♀	5	1	1	1	0	12.3 ± 0.34 (11-13)	5.9 ± 0.19 (5-7)	1	1	1	2	0	4.7 ± 0.12 (4-5)	0.90 ± 0.100 (0-1)
3rd	<i>Australomimetes spinosus</i>	♂	10	1	1	1	0	12.5 ± 0.24 (11-14)	6.5 ± 0.16 (6-8)	1	1	1	2	0	5.3 ± 0.11 (4-6)	0.05 ± 0.050 (0-1)
4th	<i>Australomimetes djuka</i>	♀	1	1	1	1	0	21.5 (21-22)	13	1	0	0	2	0	4.5 (4-5)	0
4th	<i>Australomimetes spinosus</i>	♀	5	1	1	1	0	18.3 ± 0.34 (16-19)	10.3 ± 0.25 (9-11)	1	1	1	2	0	7.8 ± 0.25 (7-9)	0.90 ± 0.245 (0-2)
4th	<i>Australomimetes spinosus</i>	♂	8	1	1	1	0	18.6 ± 1.00 (16-25)	10.9 ± 0.55 (9-14)	1	1	1	2.1 ± 0.13 (2-3)	0	7.6 ± 0.22 (6-9)	1.5 ± 0.21 (0-3)
5th Juvenile	<i>Australomimetes djuka</i>	♀	3	1	1	1	0	32.5 ± 1.53 (28-35)	19.7 ± 3.18 (16-26)	1	0	0	1.8 ± 0.17 (1-2)	0	5.8 ± 0.44 (5-7)	0
5th Adult	<i>Australomimetes djuka</i>	♂	2	1	0	1	1	30.0 ± 1.50 (28-33)	20.3 ± 1.25 (19-22)	1	0	0	2.5 ± 0.50 (2-3)	0	5.5 ± 0.50 (5-6)	0
5th Juvenile	<i>Australomimetes spinosus</i>	♀	3	1	1	1	0	27.0 ± 2.57 (22-33)	16.0 ± 1.00 (14-18)	1	1	1	2	0	9.2 ± 0.67 (8-11)	2.7 ± 0.73 (1-4)
5th Juvenile	<i>Australomimetes spinosus</i>	♂	4	1	1	1	0	25.1 ± 1.07 (22-29)	15.1 ± 1.30 (12-18)	1	1	1	2	0	9.9 ± 0.13 (9-11)	2.6 ± 0.24 (2-3)
5th Adult	<i>Australomimetes spinosus</i>	♀	2	1	0	1	1	42.8 ± 3.25 (39-46)	21	1	0	2	2.3 ± 0.25 (2-3)	0	12.0 ± 1.00 (11-13)	4.3 ± 0.25 (4-5)
5th Adult	<i>Australomimetes spinosus</i>	♂	3	1	0	1	1	31.5 ± 1.04 (28-33)	19.0 ± 1.32 (16-22)	1	0	1	3.7 ± 0.33 (3-4)	0	11.0 ± 0.58 (10-12)	4.2 ± 0.83 (2-5)
6th Adult	<i>Australomimetes djuka</i>	♀	1	1	0	1	1	45.5 (44-47)	35.5 (35-36)	1	0	0	2	0	7.5 (7-8)	0
6th Adult	<i>Australomimetes spinosus</i>	♀	2	1	0	1	1	42.5 ± 0.50 (41-44)	25.5 ± 1.00 (23-27)	1	0	1	2	0	12.3 ± 0.25 (12-13)	4.5 ± 0.50 (4-5)
6th Adult	<i>Australomimetes spinosus</i>	♂	2	1	0	1	1	35.5 ± 3.00 (32-40)	21.5 ± 2.50 (19-25)	1	0	1	4.3 ± 0.25 (4-5)	0	13.8 ± 0.25 (13-14)	5.3 ± 0.25 (5-6)

AC, aciniform silk gland; ALS, anterior lateral spinneret; CY, cylindrical silk gland; 1° MaA, primary major ampullate silk gland; 2° MaA, secondary major ampullate silk gland; 1° MiA, primary minor ampullate silk gland; 2° MiA, secondary minor ampullate silk gland; PLS, posterior lateral spinneret; PMS, posterior median spinneret.

<sup>a</sup> Numbers are per spinneret, multiply by two for number per spider. If no variation was observed, data presented as integers. Otherwise, data presented as means ± their standard errors (calculated using the means from each pair of spinnerets) and, in parentheses, ranges (across all individual spinnerets). For both species, matching color backgrounds have been applied to PI data to facilitate comparisons between PI spigots from one stadium and PI tartipores from the following stadium. In *A. spinosus*, such backgrounds have also been applied to PLS AC data to aid comparisons between AC spigots from one stadium and AC tartipores from the following stadium. Table 3 provides a more detailed breakdown of AC data in *A. spinosus*.

<sup>b</sup> N = number of sets of spinnerets (6 spinnerets/set) examined. A total of 11 *A. djuka* and 63 *A. spinosus* sets of spinnerets were examined. Reliable counts of all spigots, tartipores, and nubbins were obtained from all 66 individual *A. djuka* spinnerets and from 373 of 378 *A. spinosus* spinnerets (indeterminate counts of PI spigots and tartipores on three ALS, AC spigots and tartipores on one PLS, and AC tartipores on one PLS; not included in table).

<sup>c</sup> AL, 2° MiA tartipore positioned anterolateral relative to 2° MiA spigot (juveniles) or nubbin (adults); PM, 2° MiA spigot (juveniles) or nubbin (adults); prim., putative nonfunctional tartipore primordium.

**Table 3.** Aciniform silk gland (AC) occurrence on posterior spinnerets (PMS + PLS) of *Australomimetes spinosus*.

Instar	Sex	Australian Region <sup>c</sup>	N <sup>d</sup>	PMS <sup>b</sup>		PLS			
				Non-T-A	Anterior <sup>e</sup> T-A		Non-T-A	Posterior <sup>e</sup> T-A	
					AC spigots	AC spigots		AC tartipores	AC spigots
1st	unknown	West	6	2	0	0	3	0	0
2nd	unknown	West	13	2	0	0	3	0.12 ± 0.083 (0-1)	0
3rd	♀	West	5	2	0.10 ± 0.100 (0-1)	0	4	0.60 ± 0.187 (0-1)	0.10 ± 0.100 (0-1)
3rd	♂	West	10	2	0.30 ± 0.082 (0-1)	0	4	0.95 ± 0.050 (0-1)	0.05 ± 0.050 (0-1)
4th	♀	West	5	2	0.90 ± 0.100 (0-1)	0.20 ± 0.122 (0-1)	5	1.9 ± 0.24 (1-3)	0.70 ± 0.122 (0-1)
4th	♂	West	7	2	0.93 ± 0.071 (0-1)	0.43 ± 0.130 (0-1)	5	1.4 ± 0.07 (1-2)	0.93 ± 0.071 (0-1)
4th	♂	East	1	3	2	1	5	2	1.5 (1-2)
5th Juvenile	♀	West	2	2	1.3 ± 0.25 (1-2)	0.75 ± 0.250 (0-1)	6	1.3 ± 0.25 (1-2)	1.3 ± 0.25 (1-2)
5th Juvenile	♂	West	4	2	1.8 ± 0.14 (1-2)	1	6	2.1 ± 0.13 (2-3)	1.6 ± 0.24 (1-2)
5th Adult	♂	West	1	3	2	1	6	2	1.5 (1-2)
5th Juvenile	♀	East	1	2	2	2	6	2.5 (2-3)	2
5th Adult	♀	East	2	2.3 ± 0.25 (2-3)	2.5 ± 0.50 (2-3)	2	6	3.5 ± 0.50 (3-4)	2.3 ± 0.25 (2-3)
5th Adult	♂	East	2	4	2.5 ± 0.50 (2-3)	2	6	3	3
6th Adult	♀	West	1	2	2	1	7	3	3
6th Adult	♀	East	1	2	3	2	7	2.5 (2-3)	3
6th Adult	♂	East	2	4.3 ± 0.25 (4-5)	3.3 ± 0.25 (3-4)	2	7	3.5 ± 0.00 (3-4)	3.3 ± 0.25 (3-4)

AC, aciniform silk gland; Non-T-A, non-tartipore-accommodated; PLS, posterior lateral spinneret; PMS, posterior median spinneret; T-A, tartipore-accommodated.

<sup>a</sup> Numbers are per PMS or PLS; multiply by two for number per spider. If no variation was observed, data presented as integers. Otherwise, data presented as means ± their standard errors (calculated using the means from each pair of spinnerets) and, in parentheses, ranges (across all individual spinnerets). Matching color backgrounds have been applied to T-A PLS AC data to facilitate comparisons between spigots of T-A AC from one stadium and AC tartipores from the following stadium, with eastern and western populations considered separately.

<sup>b</sup> As the PMS AC tartipores column in Table 2 demonstrates, all PMS AC are non-T-A.

<sup>c</sup> West: *A. spinosus* from Western Australia; East: *A. spinosus* from Queensland or New South Wales.

<sup>d</sup> N = number of sets of spinnerets (6 spinnerets/set) examined. A total of 63 *A. spinosus* sets of spinnerets were examined. Reliable counts of AC spigots and tartipores were obtained from all 126 individual PMS and from 124 of 126 PLS (indeterminate counts of AC spigots and tartipores on one PLS from 6<sup>th</sup> instar adult ♀ West, and AC tartipores on one PLS from 6<sup>th</sup> instar adult ♂ East; not included in table).

<sup>e</sup> Anterior and Posterior relative to the more centrally placed column of non-T-A AC spigots on the PLS spinning field.

## Sex determination

Copulatory structures, or evidence of their development, were the primary features consulted in determining the sex of adults and penultimate instars. The sex of younger specimens, as early as 3<sup>rd</sup> instars of *A. spinosus* and 4<sup>th</sup> instars of *A. djuka*, was primarily determined by the presence (female) or absence (male) of CY spigots on PMS and PLS. As detailed in the Results ('Cylindrical silk gland...'), the full complement of CY spigots was not present in the majority of 3<sup>rd</sup> stadium female *A. spinosus*, raising the possibility that some 3<sup>rd</sup> stadium females do not exhibit any CY spigots and leaving some uncertainty in our assignment of sex for a few 3<sup>rd</sup> stadium individuals. CY spigots appear to be absent in female as well as male 1<sup>st</sup> and 2<sup>nd</sup> instars. Thus, sex was not determined for these instars.

## Results

### Conventions applied in figures and tables

*Convention 1.* Each of the three pairs of spinnerets (ALS, PMS, PLS), split midsagittally, form right/left mirror-images (in overall arrangement) of each other. Some spinnerets depicted in the figures were from the right side of the opisthosoma, some from the left. But to facilitate

comparisons, those from the right side have been flipped in Microsoft® PowerPoint® 2016 so that they also appear to be left spinnerets. Figure legends, however, state their true handedness (right, left). Figs 3–11 are divided into three groups by spinneret pair; images in Figs 3–5 show ALS, Figs 6–8 show PMS, and Figs 9–11 show PLS. Within each group, the first figure depicts the spinneret in 1<sup>st</sup> to 3<sup>rd</sup> instars of both *A. djuka* and *A. spinosus*, while the second and third figures show the same spinneret type in later instars of just *A. spinosus* and just *A. djuka*, respectively.

*Convention 2.* On each anterior lateral spinneret (ALS) and posterior lateral spinneret (PLS), spinning fields are restricted to the more distal of the two segments composing the spinneret. Posterior median spinnerets (PMS) are single-segmented with spigots apically placed. Fig. 2A provides an overview of a set of spinnerets (though the ALS and PLS from one side of the opisthosoma are only partially visible), with boxes approximating the regions and perspectives shown in Figs 3–11. For ALS and PLS, essentially only the medial face of the distal segment is shown in Figs 3–5 and Figs 2B, 9–11, respectively. For PMS, all or nearly all of the spinneret is shown in Figs 6–8, most often from a perspective roughly perpendicular to the opisthosoma surface. Note, however, that the boxed PMS in Fig. 2A depicts a right PMS whereas Figs 6–8 de-



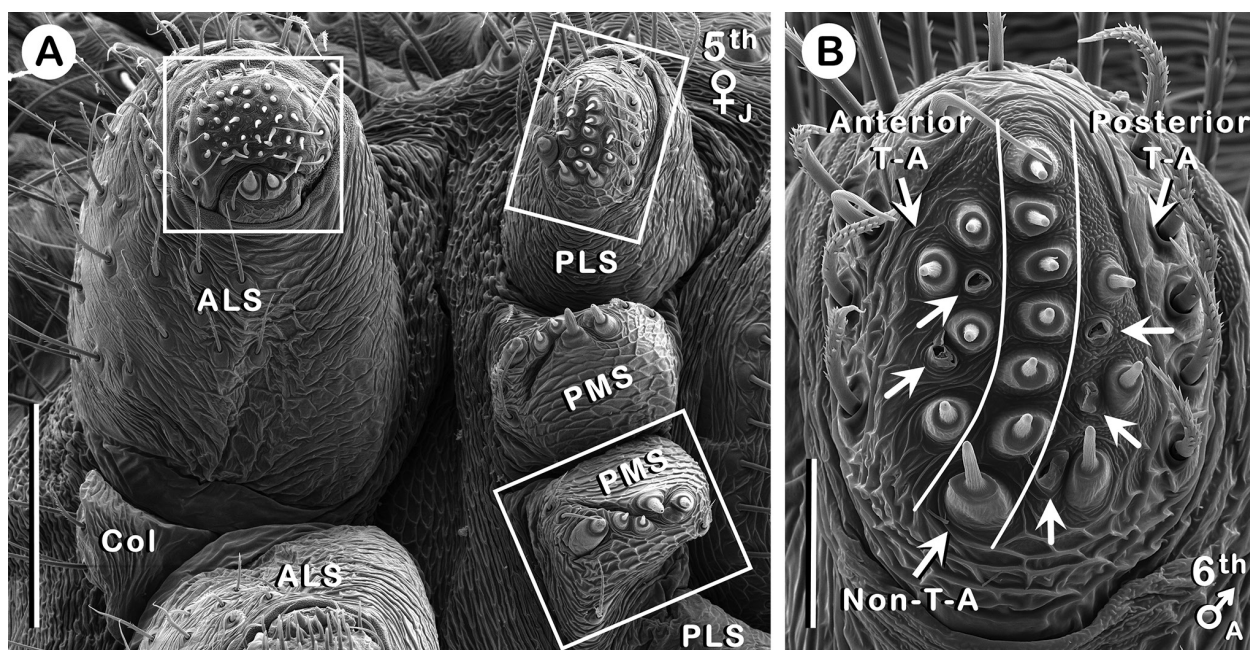


**Figure 2.** Spinnerets of *Australomimetus spinosus*. **A.** Overview of spinnerets. Boxes indicate approximate regions and perspectives shown in many of the images in Figs 3–11. Upper spinnerets from right side of opisthosoma (image flipped). **B.** Division of PLS into three AC regions: non-T-A AC (AC spigot column between two white curves), anterior T-A AC (AC spigots and tartipores left of left white curve), and posterior T-A AC (AC spigots and tartipores right of right white curve). AC tartipores indicated by unlabeled arrows. White curves in Figs 9, 10 likewise separate these three regions. Left PLS; all spigots are those of AC. Scale bars: A 100  $\mu$ m; B 20  $\mu$ m. See also Abbreviations and terminology (‘Spinning apparatus abbreviations’) and Results (Convention 3 in ‘Conventions applied...’).

pict left PMS (even though some are actually right PMS, see Convention 1).

**Convention 3.** Figures include a label indicating the instar from which the spinneret shown was obtained (1<sup>st</sup> to 6<sup>th</sup>; Ph, pharate instar) and, if known, the spider’s sex (♀, ♂) followed by a state of maturity subscript (J, juvenile; A, adult). For example, 4<sup>th</sup> ♀<sub>J</sub> indicates a juvenile female 4<sup>th</sup> instar. Sex was unknown only for 1<sup>st</sup> and 2<sup>nd</sup> instars, though uncertain for some 3<sup>rd</sup> instars [see Results (‘Cylindrical silk gland...’)].

**Convention 4.** One of the new findings of the present study is that *A. spinosus*, unlike *A. djuka* and five other *Australomimetus* species previously examined (Harms and Harvey 2009b, Townley and Tillinghast 2009), has T-A AC in addition to non-T-A AC emptying on the PLS. The T-A AC spigots and tartipores occur both anterior and posterior to a more centrally located column of non-T-A AC spigots on each PLS, as shown in the example in Fig. 2B. Thus, we make a distinction between anterior and posterior T-A AC spigots and tartipores in Table 3, Figs 2B, 9, 10, and the text.

**Convention 5.** As noted in ‘Spinnerets examined’ in Materials and methods, in only one instance were two consecutive sets of spinnerets from the same individual identified; 4<sup>th</sup> and pharate 5<sup>th</sup> instar sets from a proecdysial 4<sup>th</sup> stadium juvenile male *A. spinosus*, separated from one another during enzyme cleaning and examined separately. All of the colorized micrographs (Figs 4A, B, 7A,

B, 10A–D) are from this male’s two sets of spinnerets. The color coding is as follows:

**Red:** Spigots of non-T-A silk glands that were functional during the 4<sup>th</sup> stadium and would have been functional again during the 5<sup>th</sup> and 6<sup>th</sup> (adult) stadia, though not during proecdyses. Thus, they were not functional at the time the spider was preserved.

**Purple (Fuchsia):** Spigots of non-T-A silk glands that would have been functional for the first time during the 5<sup>th</sup> stadium, though not during proecdysis, and then again during the 6<sup>th</sup> (adult) stadium. Only certain AC spigots (Fig. 10C, D) fall into this category.

**Blue:** Spigots and tartipores of T-A silk glands that were functional during the 4<sup>th</sup> stadium, at least during proecdysis (and presumably also well prior to apolysis for at least some of these silk glands, such as PI). The PI and AC members of this group would have been functional again during the 6<sup>th</sup> (adult) stadium, while the 2<sup>o</sup> MaA and 2<sup>o</sup> MiA members would have atrophied, their spigots replaced by nubbins. In the 5<sup>th</sup> instar, the presence of these silk glands would have been indicated externally only by post-functional tartipores.

**Yellow:** Spigots and tartipores of T-A silk glands that would have been functional during the 5<sup>th</sup> stadium and had previously been functional during the 3<sup>rd</sup> stadium, at least during proecdyses (and presumably also well prior to apolysis for at least some of these silk glands, such as PI). None of these would have been functional during the

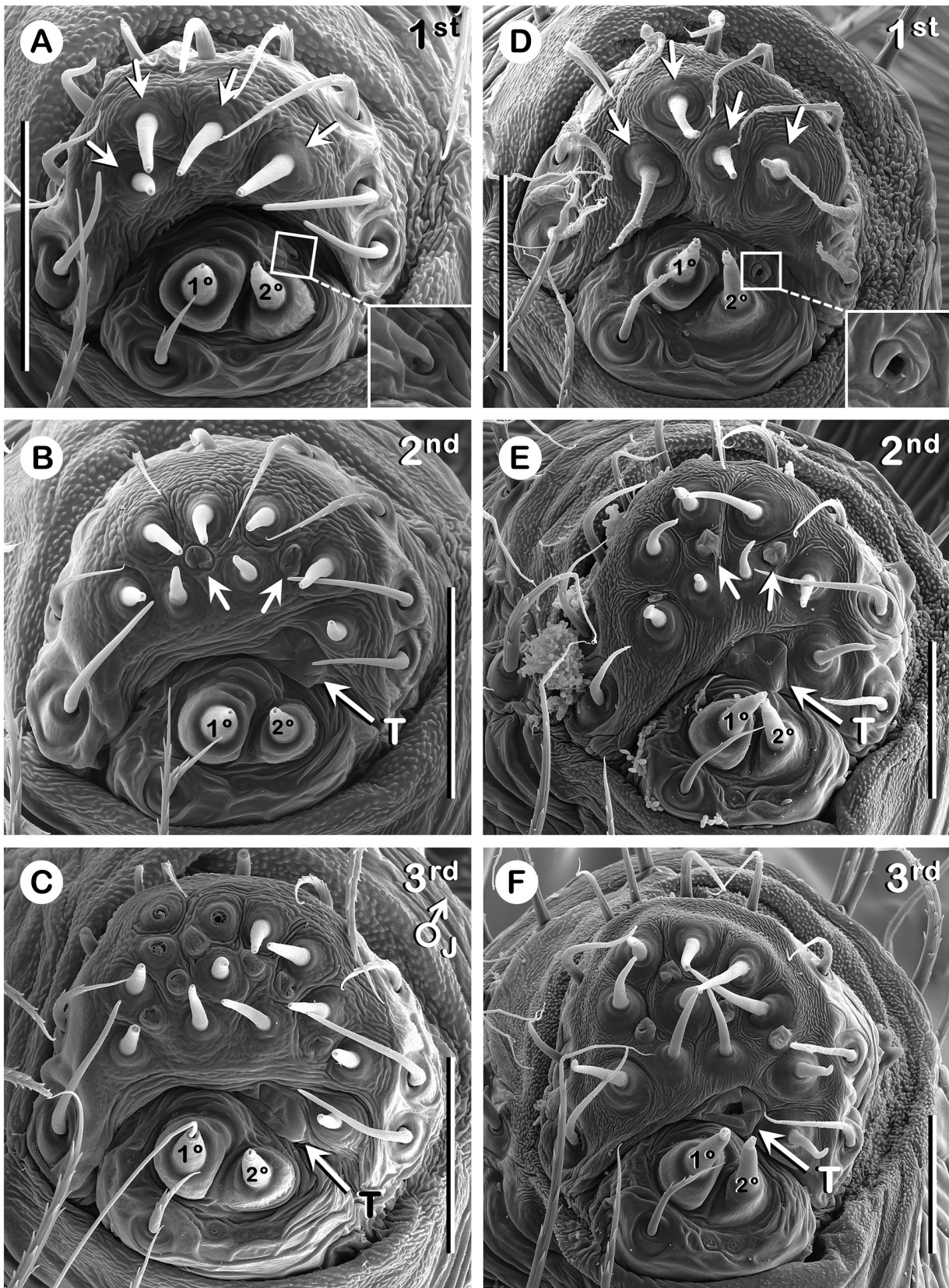


**Figure 3.** ALS of 1<sup>st</sup> to 3<sup>rd</sup> instars of *Australomimetes spinosus* and *Australomimetes djuka*. **A–C.** *A. spinosus*. **D–F.** *A. djuka*. **A, D.** Boxed regions, magnified in insets, show putative 2° MaA tartipore primordia. Unlabeled arrows indicate the four PI spigots present in 1<sup>st</sup> instars (two T-A, two non-T-A); note increased PI spigot numbers in later instars. **B, E.** Unlabeled arrows indicate the two PI tartipores present in 2<sup>nd</sup> instars; note increased PI tartipore numbers in later instars. **A, C, E, F.** Left ALS. **B, D.** Right ALS (image flipped). 1°, 1° MaA spigot; 2°, 2° MaA spigot; T, 2° MaA tartipore. All scale bars 20 μm. See also Abbreviations and terminology (‘Spinning apparatus abbreviations’) and Results (Convention 3 in ‘Conventions applied...’).

6<sup>th</sup> (adult) stadium. In the 4<sup>th</sup> instar, the presence of these silk glands was indicated externally only by post-functional tartipores.

Green: Spigots of T-A silk glands that would have been functional for the first time during the 5<sup>th</sup> stadium, at least during proecdysis (and presumably also well prior to apolysis for at least some of these silk glands, such as PI). None of these would have been functional during the 6<sup>th</sup> (adult) stadium.

**Convention 6.** Tables 2 and 3 compile spigot, tartipore, and nubbin data from all examined spinnerets that yielded reliable counts. Data for silk gland types with multiple spigots and tartipores per spinneret (at least in some stadia)—namely, PI data from both species (Table 2) and PLS AC data from *A. spinosus* (Tables 2, 3)—are color coded to guide the eye in making comparisons between spigot counts from one stadium and tartipore counts from the next. For example, in Table 2 it can be seen that in female *A. spinosus*, 3<sup>rd</sup> instars had a mean of 12.3 PI spigots/ALS and, shaded in the same color, 4<sup>th</sup> instars had 10.3 PI tartipores/ALS, consistent with two PI spigots/ALS in 3<sup>rd</sup> instars being outlets for non-T-A PI, the remainder outlets for T-A PI. PLS AC spigot and tartipore data from *A. spinosus* are presented first on a ‘counts per PLS’ basis (Table 2) and then divided on a ‘counts per PLS region’ basis (Table 3), where three regions are recognized on each PLS: an anterior T-A AC region, a central non-T-A AC region, and a posterior T-A AC region (Fig. 2B). The data in Table 3 are further segregated by geography [eastern Australia (Queensland, New South Wales)/Western Australia].

### Instar/stadium assignments and molts to maturity

Preserved spiders and exuvia were assigned to specific instars/stadia based on numbers of spigots and tartipores from the three pairs of spinnerets and, for *A. spinosus*, the position of the 2° MiA tartipore (Table 2). Though we believe at least most of these assignments are accurate, a small amount of uncertainty remains for later instars (beyond the 3<sup>rd</sup>), especially in *A. djuka*. This is because 1) there is variation in the number of molts completed before maturity is attained, 2) ranges of spigot/tartipore counts can overlap, especially between later instars, 3) we have considerably more data for *A. spinosus* than *A. djuka*, and 4) spinnerets of *A. spinosus* are more informative than those of *A. djuka* thanks to the presence of 2° MiA and T-A PLS AC in the former, but not the latter.

Based on examination of spinnerets from nine adults, both female and male *A. spinosus* have the potential to become adults after either five or six molts [Table 2; see Abbreviations and terminology (‘Terminology’) and Fig. 1 for numbering of molts, instars, stadia]. Consistent with this conclusion, palps swollen to different extents indicated that one of eight male 4<sup>th</sup> instars was in the penultimate stadium, the rest in the antepenultimate stadium, and all four juvenile male 5<sup>th</sup> instars were in the penultimate stadium. With data from only three *A. djuka* adults, we can

only say that at least some males become adults after five molts and at least some females become adults after six molts. Consistent with this finding, all three juvenile 5<sup>th</sup> instars examined were females (Table 2). For both species, but especially *A. djuka*, examinations of additional specimens could very well reveal greater variability with respect to the number of molts to maturity for one or both sexes. Overall, there seems to be some variability regarding the number of molts to maturity, with food availability and space being potential factors determining the number of molts.

### Anterior Lateral Spinnerets (ALS)

Contrary to what was observed on the other two pairs of spinnerets, described below, there were no substantial differences between ALS of *A. spinosus* and *A. djuka*. Both had single 1° and 2° MaA spigots on each ALS in all instars, with the exception that the 2° MaA spigot was replaced by a 2° MaA nubbin in adults (Table 2, Figs 3–5). Such nubbins were thus ontogenetic nubbins. Both species had four PI spigots/ALS in all examined 1<sup>st</sup> instars (Table 2, Fig. 3A, D) that were outlets for two T-A PI and two non-T-A PI, as demonstrated by two PI tartipores/ALS in all 2<sup>nd</sup> instars (Table 2, Fig. 3B, E). With each molt, numbers of PI spigots and tartipores increased (Table 2, Figs 3–5), but the number of non-T-A PI very likely remained constant (two/ALS) through all stadia. The best evidence for this came from a proecdysial 4<sup>th</sup> stadium male *A. spinosus* [see Results (Convention 5 in ‘Conventions applied...’)] that allowed us to compare the right ALS on both old (Fig. 4A) and new (Fig. 4B) exoskeletons (the left ALS of the old exoskeleton was too damaged for such a comparison). Of 16 PI spigots on the 4<sup>th</sup> instar’s old exoskeleton (Fig. 4A, blue and red PI spigots), 14 (blue) could be paired with 14 PI tartipores in the pharate 5<sup>th</sup> instar’s exoskeleton (Fig. 4B, blue PI tartipores), leaving two non-T-A PI spigots (Fig. 4A, red PI spigots) that, though non-functional during proecdysis, were functional earlier in the 4<sup>th</sup> stadium and would have been functional after ecdysis during the 5<sup>th</sup> stadium (Fig. 4B, red PI spigots).

When PI spigot numbers in specimens at one stadium were compared with PI tartipore numbers in specimens at the next stadium, there were further indications of a constant two non-T-A PI/ALS in all instars. For example, in *A. spinosus*, PI spigots in 13 2<sup>nd</sup> instars and PI tartipores in 15 3<sup>rd</sup> instars numbered from 7–10 ( $\bar{Y} = 8.2$ )/ALS and 5–8 ( $\bar{Y} = 6.3$ )/ALS, respectively (Table 2). Another such comparison between 3<sup>rd</sup> and 4<sup>th</sup> instars of *A. spinosus* was noted earlier [Results (Convention 6 in ‘Conventions applied...’)]. Not all of these comparisons suggested constancy in the number of non-T-A PI across stadia, but this can probably be attributed to variation in the number of T-A PI at each stadium and the low number of observations involved in some comparisons.

In the proecdysial 4<sup>th</sup> stadium male *A. spinosus*, nine PI tartipores were present in the old exoskeleton (Fig. 4A,

yellow PI tartipores), indicating the positions of T-A PI spigots in the exoskeleton of the 3<sup>rd</sup> instar. Interestingly, a group of nine PI spigots in the pharate 5<sup>th</sup> instar's exoskeleton (Fig. 4B, yellow PI spigots) were arranged, relative to one another and to the two non-T-A PI spigots (red), very much like the PI tartipores in the 4<sup>th</sup> instar. This is compelling evidence that the same T-A PI that functioned during the 3<sup>rd</sup> stadium were about to return to service during the 5<sup>th</sup> stadium, and, by extension, that two of these nine T-A PI had functioned for the first time during the 1<sup>st</sup> stadium. In keeping with the number of T-A PI spigots increasing after each molt (Table 2, Figs 3–5), the pharate 5<sup>th</sup> instar's ALS contained, in addition to spigots of the nine returning T-A PI (Fig. 4B, yellow), 13 spigots of T-A PI (Fig. 4B, green) that were about to function, apparently for the first time, during the 5<sup>th</sup> stadium. These were located at the periphery of the PI spinning field.

In Fig. 4A, B, the spigot of the 1<sup>o</sup> MaA has been colored red to emphasize that this silk gland was non-T-A, like the two red-colored non-T-A PI associated with each ALS; all three apparently functional during every stadium and at all times except during proecdysis. Likewise, spigots and tartipores of 2<sup>o</sup> MaA have been colored blue or yellow to emphasize that they were T-A, like the blue- or yellow-colored T-A PI, and were functional at least during proecdysis. Any single T-A silk gland, however, functioned only during alternate stadia, i.e., either during even-numbered stadia (Fig. 4A, blue), with an accommodating tartipore forming in odd-numbered pharate instars (Fig. 4B, blue), or during odd-numbered stadia (Fig. 4B, yellow), with an accommodating tartipore forming in even-numbered pharate instars (which, in the case of the silk glands indicated in yellow in Fig. 4B, would have been the pharate 6<sup>th</sup> instar, just as the yellow tartipores in Fig. 4A had earlier formed in the pharate 4<sup>th</sup> instar to accommodate silk glands functioning during proecdysis in the 3<sup>rd</sup> stadium). Two colors (blue, yellow) thus signify different groups of silk glands functioning in alternation with one another.

Postembryos were not examined, but all indications were that functional spigots first appeared in 1<sup>st</sup> instars. Thus, in both species, PI and 2<sup>o</sup> MaA tartipores first appeared in the exoskeletons of 2<sup>nd</sup> instars (Fig. 3B, E). MaA spinning fields of 1<sup>st</sup> instars contained a structure we interpret to be a 2<sup>o</sup> MaA tartipore primordium (Fig. 3A, D). These occupied positions similar to those taken by 2<sup>o</sup> MaA tartipores in the exoskeletons of 2<sup>nd</sup> (Fig. 3B, E) and later instars (Figs 3C, F, 4, 5), and were only observed in the exoskeletons of 1<sup>st</sup> instars. Though generally round and containing a depression or pore, the precise appearance of these presumed primordia varied within each species and within individuals. We do not attach significance to the difference in morphology exhibited in the examples shown in Fig. 3 A, D.

In some mimetid males, maturity brings the appearance of a pair of modified PI (MoPI) spigots to each ALS that differ morphologically from the other PI (Townley and Tillinghast 2009, Townley et al. 2013, Benavides and Hormiga 2016). It has been hypothesized that the two pairs of non-T-A PI, functional from the 1<sup>st</sup> stadium,

transform in the pharate final instar into the MoPI, such that their spigots at least, and presumably their corpora as well, become recognizably different from those of other PI (Townley and Tillinghast 2009, Townley et al. 2013). In none of the adult males examined in this study (five *A. spinosus*, two *A. djuka*) were MoPI spigots observed. Representative ALS from adult male *A. spinosus* and *A. djuka* are shown in Figs 4D, E, 5B, C, respectively, with spigots in the positions of non-T-A PI spigots indicated by stars. These showed no obvious differences to surrounding T-A PI spigots, nor to non-T-A PI spigots in adult females of these species (Figs 4F, G, 5D, E, respectively).

### Posterior Median Spinnerets (PMS) – General description

PMS of the two species differed from the 1<sup>st</sup> stadium. In *A. djuka*, 1<sup>st</sup> and 2<sup>nd</sup> instars had one AC spigot/PMS, increasing to two in a 3<sup>rd</sup> instar, while *A. spinosus* invariably started off with two AC spigots/PMS in 1<sup>st</sup> instars (Table 2, Fig. 6A, E–H). These and all PMS AC in both species were non-T-A. More significant were differences in MiA complements. Both species had a single 1<sup>o</sup> MiA spigot on each PMS from the 1<sup>st</sup> to the final stadium, but only *A. spinosus* also had one 2<sup>o</sup> MiA spigot/PMS at all juvenile stadia (Table 2, Figs 6–8). Observations on the 2<sup>o</sup> MiA in *A. spinosus* matched those of the 2<sup>o</sup> MaA: 1) the 2<sup>o</sup> MiA spigot was replaced by an ontogenetic 2<sup>o</sup> MiA nubbin in adults (Fig. 7C, D, F), 2) a 2<sup>o</sup> MiA tartipore first appeared in 2<sup>nd</sup> instars (Fig. 6B), and 3) a structure we interpret to be a 2<sup>o</sup> MiA tartipore primordium was adjacent to the 2<sup>o</sup> MiA spigot on the PMS of all 1<sup>st</sup> instars (Fig. 6A), but no later instars (Figs 6B–D, 7). Nor was such a structure seen on PMS of 1<sup>st</sup> instars of *A. djuka* (Fig. 6E, F).

The absence of functional 2<sup>o</sup> MiA in all examined specimens of *A. djuka* appears to represent a secondary loss: an apparent phylogenetic 2<sup>o</sup> MiA nubbin was observed on all four examined PMS from two 1<sup>st</sup> instars of *A. djuka* (Table 2, Fig. 6E, F). This nubbin occupied the same position taken by the 2<sup>o</sup> MiA spigot in 1<sup>st</sup> instars of *A. spinosus* (cf. Fig. 6A, E) and was not observed in later instars (Figs 6G, H, 8A–D).

On both old and new exoskeletons from the proecdysial 4<sup>th</sup> stadium male *A. spinosus* [see Results (Convention 5 in 'Conventions applied...')], spigots of non-T-A silk glands on each PMS included all (two) AC spigots and the 1<sup>o</sup> MiA spigot (Fig. 7A, B, red). These silk glands were nonfunctional during this and earlier proecdyses, but were potentially functional between ecdysis and apolysis during this and all previous stadia and would have been functional again during the 5<sup>th</sup> and 6<sup>th</sup> (adult) stadia. The only T-A silk glands were two 2<sup>o</sup> MiA associated with each PMS, one functional during proecdyses of the 2<sup>nd</sup> and 4<sup>th</sup> stadia (Fig. 7A, blue), the other functional during proecdyses of the 1<sup>st</sup>, 3<sup>rd</sup>, and (upcoming) 5<sup>th</sup> stadia (Fig. 7B, yellow). This arrangement again matched that of ALS-associated 2<sup>o</sup> MaA. The blue 2<sup>o</sup> MiA tartipore in Fig. 7B was accommodating the duct of the 2<sup>o</sup> MiA

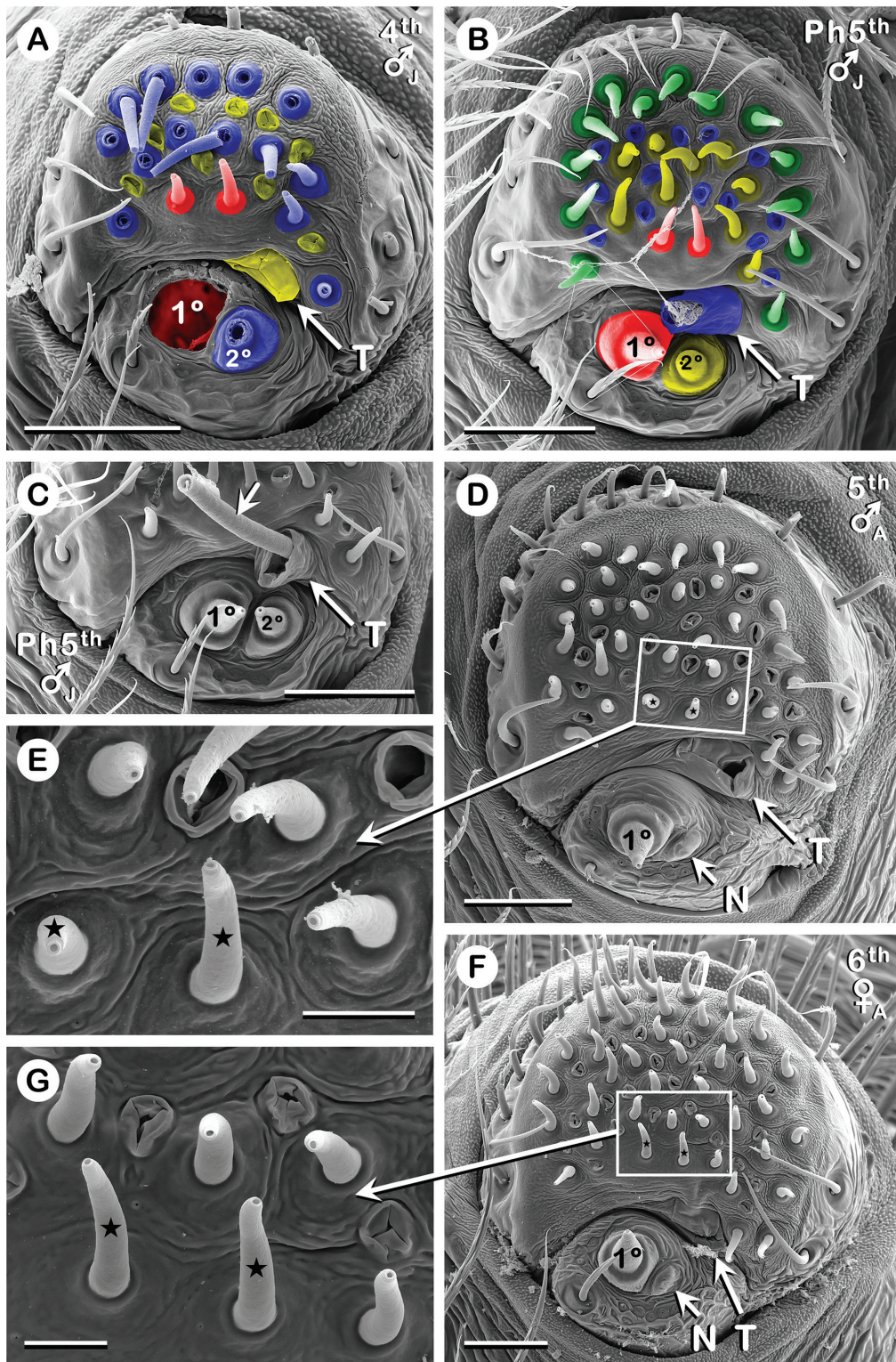


**Figure 4.** ALS of 4<sup>th</sup> to 6<sup>th</sup> instars of *Australomimetes spinosus*. A-C. ALS from one juvenile specimen, well into proecdysis. Color coding explained in Results (Convention 5 in ‘Conventions applied...’). A. Old exoskeleton (all spigots but one damaged; 1° MaA spigot torn out entirely, but its former location is colored red). B. New exoskeleton directly beneath (A). C. New exoskeleton, opposite ALS from (A, B), demonstrating utility of a tartapore. Unlabeled arrow to 2° MaA duct (severed at distal end) still accommodated by 2° MaA tartapore (T). Before old and new exoskeletons were separated, this duct emptied on a 2° MaA spigot on old exoskeleton (like that in (A) but on opposite ALS). D-G. Adults. Presumed pair of non-T-A PI spigots (stars) on each ALS in males (D, E) were morphologically similar to T-A PI spigots (unlabeled PI spigots) in both sexes and to non-T-A PI spigots (stars) in females (F, G): no MoPI spigots. C. Left ALS. A, B, D-G. Right ALS (image flipped). 1°, 1° MaA spigot; 2°, 2° MaA spigot; N, 2° MaA nubbin (ontogenetic); T, 2° MaA tartapore. Scale bars: A-D, F 20 µm; E, G 5 µm. See also Abbreviations and terminology (‘Spinning apparatus abbreviations’) and Results (Convention 3 in ‘Conventions applied...’).

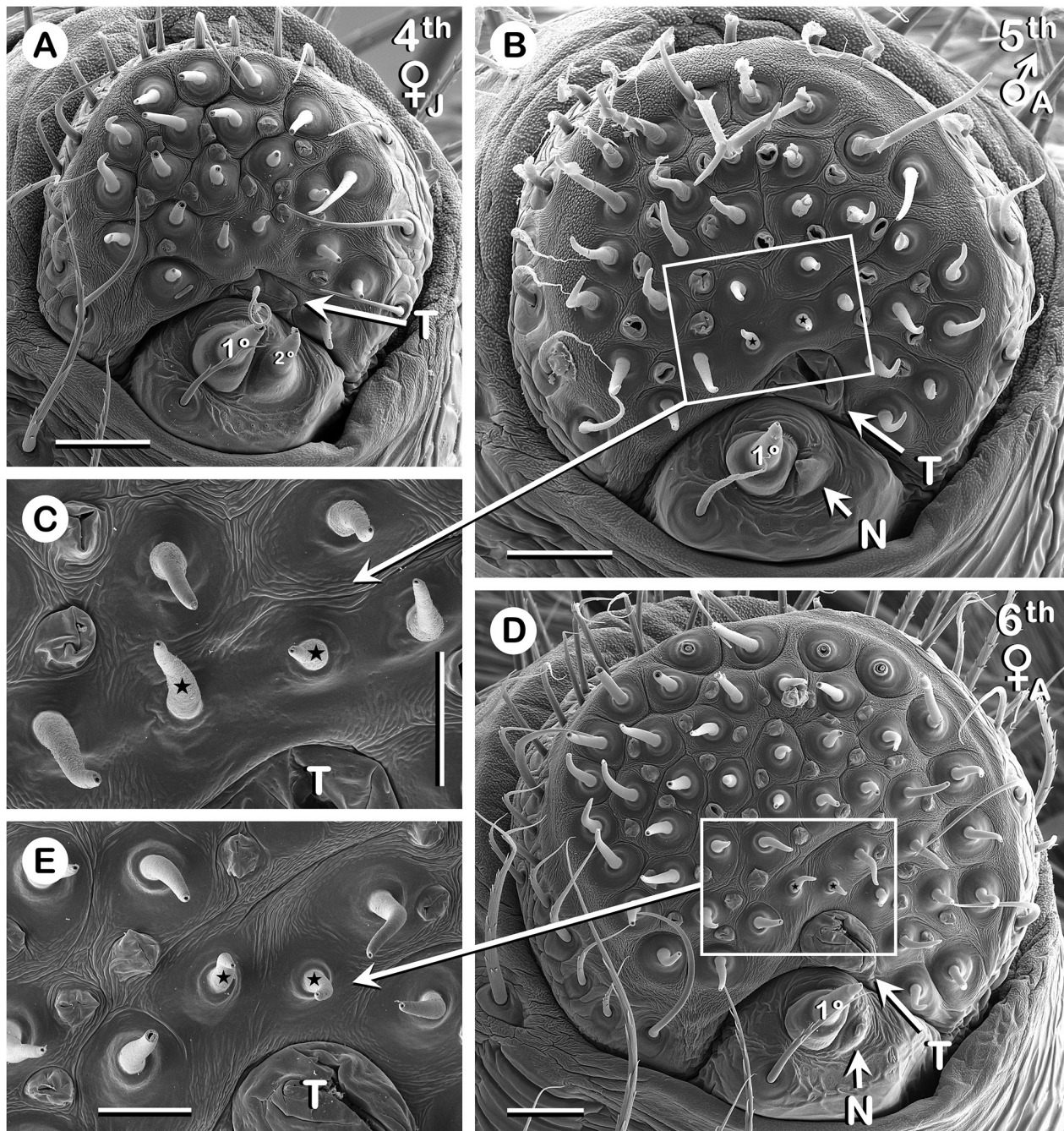


**Figure 5.** ALS of 4<sup>th</sup> to 6<sup>th</sup> instars of *Australomimetes djuka*. **A.** Juvenile. **B–E.** Adults. Presumed pair of non-T-A PI spigots (stars) on each ALS in males (**B, C**) were morphologically similar to T-A PI spigots (unlabeled PI spigots) in both sexes and to non-T-A PI spigots (stars) in females (**D, E**): no MoPI spigots. **A, D, E.** Left ALS. **B, C.** Right ALS (image flipped). 1°, 1° MaA spigot; 2°, 2° MaA spigot; N, 2° MaA nubbin (ontogenetic); T, 2° MaA tartipore. Scale bars: A, B, D 20 µm; C, E 10 µm. See also Abbreviations and terminology (‘Spinning apparatus abbreviations’) and Results (Convention 3 in ‘Conventions applied...’).

functioning during this 4<sup>th</sup> stadium proecdysis, while the yellow 2° MiA tartipore in Fig. 7A had accommodated the other 2° MiA during proecdysis in the 3<sup>rd</sup> stadium.

#### Posterior Median Spinnerets (PMS) – Sexual and geographic dimorphism

AC associated with the PMS appeared to present an example of sexual dimorphism in *A. spinosus*, though

examination of additional specimens will be needed to establish the consistency of certain details. With one exception, the number of AC spigots in females was a constant two/PMS at all stadia (Table 3, Figs 6C, 7C). Adult males and one 4<sup>th</sup> (antepenultimate) stadium male, in contrast, had between 3–5 AC spigots/PMS (Table 3). The additional AC spigots in these males (hereafter ‘late AC spigots’) were anterior to the two AC spigots present from the 1<sup>st</sup> stadium (hereafter ‘pioneer AC spigots’)

(Fig. 7D–G), close to the position of the CY spigot in females (Fig. 7C). Late AC spigot morphology did not differ greatly from that of pioneer AC spigots, though in the single examined adult male from Western Australia (with three AC spigots on each PMS, Table 3), the distal end of the base of the late AC spigot was narrower and with a less pronounced rim than those of the pioneer AC spigots (Fig. 7G). One consistent morphological difference between late and pioneer AC spigots was a wider opening on the late AC spigots (Fig. 7E, G). This applied to all six males that had at least three AC spigots/PMS (which included all five examined adult males), one from Western Australia, five from eastern Australia (Table 3). The single exceptional female was a 5<sup>th</sup> stadium adult that had three AC spigots on one PMS (two on the other PMS), with the late AC spigot separated from the pioneer AC spigots by a gap (about the diameter of an AC spigot) not seen in any male. As in males, the opening of the late AC spigot was wider than those of the pioneer AC spigots.

AC spigot data from *A. djuka* did not suggest a clear sexual dimorphism like that indicated in *A. spinosus*, though there were some similarities. Females, including the single adult female examined, usually had two AC spigots/PMS and never exceeded this number (Table 2, Fig. 8A–C). In contrast, one of two examined adult males had three AC spigots on each PMS (Fig. 8D), with the distal end of the base of the late AC spigot narrower than those of the pioneer AC spigots (Fig. 8E). However, no difference was apparent in the width of the openings of late versus pioneer AC spigots (Fig. 8E) and, moreover, the other adult male only had two AC spigots on each PMS (Table 2).

The PMS AC data also suggested a difference among males of *A. spinosus* by geography. Again, it will be necessary to examine more specimens to better evaluate this difference, but the data obtained thus far were consistent in indicating that late stadium males from eastern Australia have more AC spigots/PMS than males from Western Australia (Table 3).

Observations pertaining to PMS CY are presented below.

### Posterior Lateral Spinnerets (PLS)

As with PMS-associated AC, the two species differed during the earliest stadia with respect to the number of non-T-A AC spigots/PLS: two in 1<sup>st</sup> and 2<sup>nd</sup> instars of *A. djuka* (Fig. 9A, B), increasing to three for the 3<sup>rd</sup> stadium (Fig. 9C), as compared with three already present in 1<sup>st</sup> instars of *A. spinosus* (Fig. 9D, Table 2). However, a more significant difference between the two species emerged as early as the 2<sup>nd</sup> stadium, though more often the 3<sup>rd</sup>, with the appearance of T-A AC spigots in *A. spinosus* (Table 3). In both species there were modest increases in the number of AC spigots/PLS over a spider's ontogeny, but in *A. djuka* these increases consisted solely of additional non-T-A AC spigots (Table 2, Fig. 11). In *A. spinosus*, both non-T-A and T-A AC spigots were added to the PLS spinning field, with the non-T-A AC spigots forming a central column in

the field, albeit with a slight-to-pronounced anterior displacement at the proximal end of the column (e.g., Figs 2B, 9I) and/or with the second spigot from the proximal end displaced posteriorly (e.g., Figs 9L, 10C). T-A AC spigots occurred both anterior and posterior to the non-T-A AC spigot column (Fig. 2B). Beginning with the ecdysis between the 2<sup>nd</sup> and 3<sup>rd</sup> stadia, the number of non-T-A AC spigots increased from one stadium to the next in both species: in *A. spinosus*, this increase was invariably one/PLS (Table 3), while in *A. djuka* the increase was variable with, in some instances, at least two such spigots apparently added to a PLS following a molt (Table 2, also cf. Fig. 11B–E, all 5<sup>th</sup> instars). Intra-stadium variability in AC spigot number in *A. spinosus* was confined to T-A AC spigots (Table 3). In both species, angularities in the column formed by the non-T-A AC spigots could be present (e.g., Figs 10C, 11A) or absent (e.g., Figs 2B, 11B), but were more often present in *A. djuka*.

Most 2<sup>nd</sup> stadium PLS of *A. spinosus* (23 of 26 PLS from 13 2<sup>nd</sup> instars) had the same spinning complement as 1<sup>st</sup> stadium PLS: three non-T-A AC spigots (Fig. 9E). But the other three PLS (two from the same set of spinnerets) had, in addition, a single T-A AC spigot, consistently positioned posterior to the non-T-A AC spigot column and more distal than two of the three non-T-A AC spigots (Table 3, Fig. 9F). The identification of this AC spigot as T-A implies that we observed a similarly-positioned AC tartipore in a similarly low percentage of 3<sup>rd</sup> stadium PLS. Indeed, 28 of 30 PLS from 15 3<sup>rd</sup> instars contained no AC tartipores, but the other two PLS (on different sets of spinnerets) each had one AC tartipore, posterior to the non-T-A AC spigot column and more distal than two of the four non-T-A AC spigots (Table 3, Fig. 9G). This AC tartipore's position indicated that the spigot serving the newest (fourth) non-T-A AC was the most distal one in the column. The two exceptional 3<sup>rd</sup> stadium PLS departed further from the norm by being two of only four 3<sup>rd</sup> stadium PLS containing no T-A AC spigots (Fig. 9G). The other 26 PLS had one (Fig. 9H) or two (Fig. 9I) T-A AC spigots (Tables 2, 3).

Consistent with the prevalence of one or two T-A AC spigots on 3<sup>rd</sup> stadium PLS, one (Fig. 10A, yellow) and two (Fig. 10B, yellow) AC tartipores were found on the right and left PLS, respectively, of the old exoskeleton from the proecdysial 4<sup>th</sup> stadium male *A. spinosus* [see Results (Convention 5 in 'Conventions applied...')]. It appeared that the AC accommodated by these tartipores, functional during the 3<sup>rd</sup> stadium, would have been functional again during the 5<sup>th</sup> stadium, as evidenced by AC spigots in essentially the same locations on the new exoskeleton of this individual (Fig. 10C, D, yellow). Spigots of T-A AC functional during the 4<sup>th</sup> stadium are shown in blue in Fig. 10A, B and the tartipores accommodating them during this proecdysis are likewise shown in blue in Fig. 10C, D, respectively. Spigots of T-A AC that would have functioned for the first time during the 5<sup>th</sup> stadium are shown in green in Fig. 10C, D. Though we observed intra-stadium variation in the number of T-A

AC associated with a PLS (Tables 2, 3), including within the same individual (Fig. 10A, B), consistencies in the positions taken by their spigots were also often observed. For example, the posterior T-A AC spigot common to Fig. 9F, H, I occurred in essentially the same location relative to non-T-A AC spigots; likewise for single anterior and posterior T-A AC spigots common to Figs 9I, 10A, B. The distribution of T-A AC spigots, anterior and posterior to the non-T-A AC spigot column, also tended to be consistent. For example, there were 12 4<sup>th</sup> stadium PLS that had three T-A AC spigots (as in Fig. 10B): these were invariably distributed one anterior and two posterior. And all eight 5<sup>th</sup> stadium PLS with four T-A AC spigots (as in Fig. 10C, D) had them distributed two anterior and two posterior, while all six 5<sup>th</sup> stadium PLS with five T-A AC spigots had them distributed two anterior and three posterior.

Positions of T-A AC spigots and tartipores, relative to non-T-A AC spigots, in Fig. 10A–D again indicated that the addition of one non-T-A AC spigot to each PLS with each molt (starting with the 3<sup>rd</sup> molt) in *A. spinosus* occurs at the distal end of the non-T-A AC spigot column. Thus, in Fig. 10C, D, the spigot of the newest non-T-A AC, which would have functioned for the first time during the 5<sup>th</sup> stadium, is shown in purple (fuchsia) at the distal end of this column, while spigots of the five older non-T-A AC, functional at least by the 4<sup>th</sup> stadium and again during the 5<sup>th</sup> stadium, are shown in red in Fig. 10A–D.

Morphological differences between T-A and non-T-A AC spigots in *A. spinosus* were modest: the former sometimes had narrower bases than the latter, especially during earlier stadia (e.g., Fig. 9F, J). More consistent was a difference in the width of their openings, with those of T-A AC spigots wider. Absolute values of aperture diameters varied enough among different specimens, even within the same stadium, that diameters of non-T-A AC in one specimen sometimes overlapped with diameters of T-A AC in another specimen (cf. Fig. 9J, K), but within a specimen the T-A AC spigot openings were usually wider. Three examples are presented in Figs 9J, K, 10E, F.

Geographical differences between eastern and western populations of *A. spinosus* with respect to PLS were also modest and, as with geographical differences noted above for PMS AC, will need to be confirmed or negated by examining more material. The data currently available indicate that, from as early as the 3<sup>rd</sup> stadium (based on AC tartipore counts in 4<sup>th</sup> instars), eastern *A. spinosus* have higher mean counts of T-A AC than their western counterparts (Table 3).

No spigots of aggregate or flagelliform silk glands (AG, FL) were observed on any of the 22 *A. djuka* PLS and 126 *A. spinosus* PLS that were examined. However, a possible phylogenetic nubbin was present on the right PLS of one 4<sup>th</sup> stadium female *A. spinosus*, in a position consistent with the AG-FL triad of typical araneoids (Fig. 9L). It was adjacent to a putative sensillum. Such sensilla, roughly round to oblong and containing one (not always well-defined) raised-rim pore, could be found in essen-

tially the same location on most of the examined PLS, but with no adjacent nubbin. These are indicated in several of the micrographs shown in Figs 9–11 (labeled ‘S’).

Observations pertaining to PLS CY are presented below.

### Cylindrical silk gland (CY) spigots

In both species, a full complement of CY spigots, restricted to females, consisted of four CY spigots; one on each PMS and PLS.

In *A. spinosus*, CY spigots were first seen in 3<sup>rd</sup> instars (Figs 6C, 9H). However, only one of five 3<sup>rd</sup> stadium females had the full complement of CY spigots; the other four females had one to three CY spigots, with those on PMS especially prone to being absent (Table 2). Given the occurrence of one 3<sup>rd</sup> stadium female with only one CY spigot (on the right PLS), there may exist 3<sup>rd</sup> stadium females that take a paucity of CY spigots one spigot further and lack CY spigots entirely. If so, then one or more of the 10 3<sup>rd</sup> stadium males included in Tables 2 and 3 may actually have been female since we relied primarily on the presence or absence of CY spigots to distinguish the sexes. Six of these 10 were intact specimens with subtly swollen palps also indicating they were males; the other four, however, were exuvia on which palps were not examined and were lost during spinneret preparation. All 4<sup>th</sup> stadium and later females had the full complement of CY spigots (Table 2).

In *A. djuka*, because of the small number of early juveniles examined, we can only say that CY spigots are present at least by the 4<sup>th</sup> stadium: the only 4<sup>th</sup> instar examined had the full complement of CY spigots (Figs 8A, 11A), as did later females (Table 2). The only 3<sup>rd</sup> instar examined lacked CY spigots, and its palps, not even subtly swollen, indicated it was a female. However, since we are not certain of the sex, no conclusions can be drawn regarding the occurrence of CY spigots in 3<sup>rd</sup> stadium females of *A. djuka*.

In both species, increases in widths of CY spigots (bases and shafts) over successive stadia were disproportionately large compared with increases in nearby AC spigots [cf. Figs 6C (inset), 7H–J; Fig. 8A–C (insets); Fig. 10G–I; Fig. 11A, C, F (insets)]. The single largest increase occurred in shafts of CY spigots with passage from the penultimate to the adult stadium. The wide opening characteristic of mimetine CY spigots was restricted to adult females and the deep incisions present in CY spigot shafts of some mimitines were absent in both species (Figs 7C, J, 8C, 10E, I, 11F). However, shafts differed between the two species in two respects: 1) those of *A. djuka* were smoother, marked only by fine longitudinal striations (Figs 8C, 11F), while those of *A. spinosus* occupied a middle ground in terms of incising, having fine striations but also what might be described as modest incisions (Figs 7C, J, 10E, I), and 2) viewed from the side, *A. spinosus* shafts exhibited the domed, convex shape typical of mimetine CY spigots (Figs 7J, 10I) while *A. djuka* shafts were a little less rotund [Figs 8C, 11F (insets)].



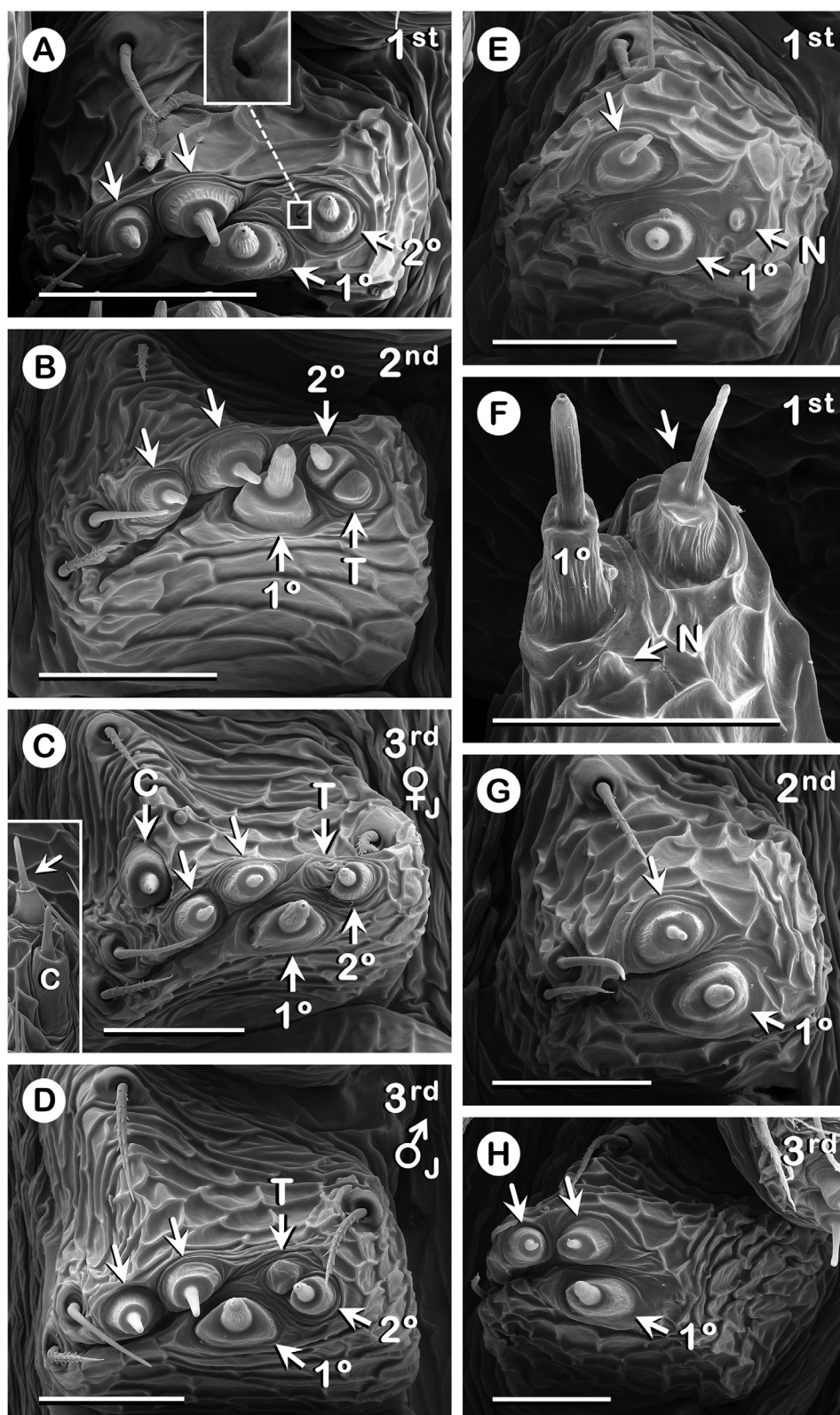


**Figure 6.** PMS of 1<sup>st</sup> to 3<sup>rd</sup> instars of *Australomimetus spinosus* and *Australomimetus djuka*. All unlabeled arrows point to non-T-A AC spigots. **A–D.** *A. spinosus*. **A.** Boxed region, magnified in inset, shows putative 2° MiA tartipore primordium. **B–D.** 2° MiA spigot (2°) and 2° MiA tartipore (T) switched positions from 2<sup>nd</sup> to 3<sup>rd</sup> stadium. This switching continued in later stadia (Fig. 7). **C.** CY spigots first appeared in 3<sup>rd</sup> instars of *A. spinosus*. Same CY spigot (C) and closest AC spigot (unlabeled arrow) shown from two perspectives. **E–H.** *A. djuka*. **E, F.** Same PMS shown from two perspectives. Note phylogenetic 2° MiA nubbin (N) in position occupied by 2° MiA spigot in *A. spinosus* (A). **B, C, E, F.** Left PMS. **A, D, G, H.** Right PMS (image flipped). 1°, 1° MiA spigot; 2°, 2° MiA spigot; C, CY spigot; N, 2° MiA nubbin (phylogenetic); T, 2° MiA tartipore. All scale bars 20 μm. See also Abbreviations and terminology (‘Spinning apparatus abbreviations’) and Results (Convention 3 in ‘Conventions applied...’).

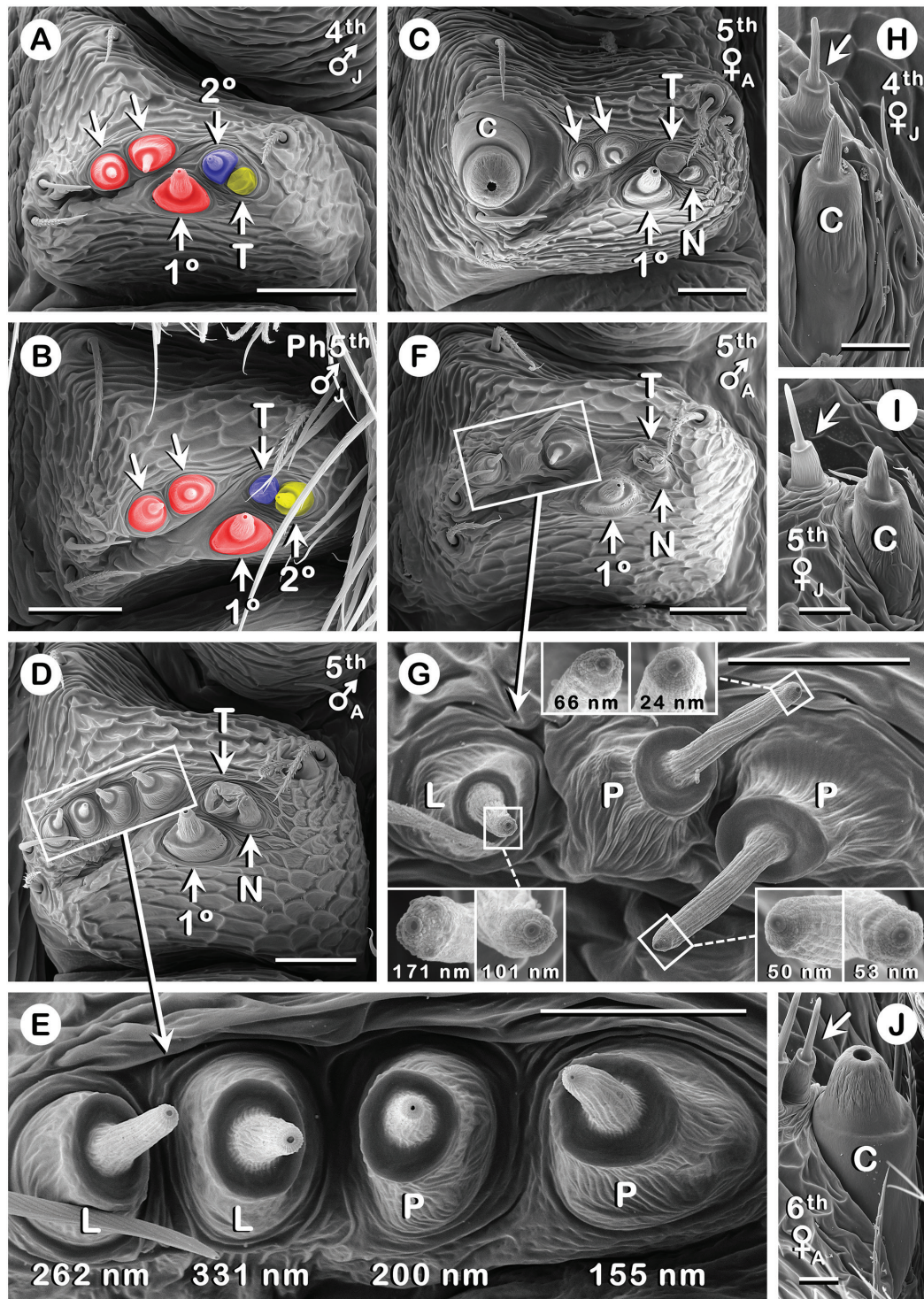


**Figure 7.** PMS of 4<sup>th</sup> to 6<sup>th</sup> instars of *Australomimetes spinosus*. All unlabeled arrows point to non-T-A AC spigots. **A, B.** PMS from one juvenile specimen, well into proecdysis. Color coding explained in Results (Convention 5 in ‘Conventions applied...’). **A.** Old exoskeleton. **B.** New exoskeleton directly beneath (A). **C.** Adult female. With one exception [see Results (‘PMS-Sexual and geographic...’) and Discussion (‘AC spigot numbers...’)], adult females had two AC spigots/PMS. **D–G.** Adult males from eastern Australia (New South Wales) (**D, E**) and Western Australia (**F, G**). AC spigots magnified in (**E, G**) to show wider openings on ‘late’ AC spigots (L) relative to neighboring ‘pioneer’ AC spigots (P) [see Results (‘PMS-Sexual and geographic...’)]; measured diameters of openings given in nm [see Materials and methods (‘SEM of spinnerets...’)]. In (**G**), distal ends of AC spigot shafts magnified in insets (connected by dashed lines), with each spigot’s counterpart on the opposite PMS shown in an adjacent inset. **H–J.** Ontogenetic changes in CY spigot (C) morphology; lateral view. Note changes in width relative to nearest AC spigot (arrow). **A–G, I, J.** Left PMS. **H.** Right PMS (image flipped). 1°, 1° MiA spigot; 2°, 2° MiA spigot; C, CY spigot; L, ‘late’ AC spigot; N, 2° MiA nubbin (ontogenetic); P, ‘pioneer’ AC spigot; T, 2° MiA tartipore. Scale bars: A–D, F 20 µm; E, G–J 10 µm. See also Abbreviations and terminology (‘Spinning apparatus abbreviations’) and Results (Convention 3 in ‘Conventions applied...’).

## Discussion

### Variable aciniform and minor ampullate silk gland (AC, MiA) characters among *Australomimetes* species

The presence of PLS AC tartipores in *A. spinosus* (Fig. 10), which signify the presence of T-A AC and an ability to draw AC silk during proecdysis, extends the range of PLS spinning field character states known for the genus *Australomimetes*. AC tartipores on the PLS have been apparent in five species of *Mimetes* (Platnick and Shadab 1993, Griswold et al. 2005, Townley and Tillinghast 2009), two species of *Phobetinus* (Townley et al. 2013), and two species of the newly described mimetid genus *Anansi* (Benavides et al. 2016), but in none of seven species of *Ero* (Platnick and Shadab 1993, Schütt 2000, Townley and Tillinghast 2009) or five earlier-examined species of *Australomimetes* (Harms and Harvey 2009b, Townley and Tillinghast 2009). The latter included *A. aurioculatus*, *A. diabolicus*, *A. maculosus*, *A. pseudomaculosus*, and *A. tasmaniensis*, to which we can now add *A. djuka* (Fig. 11). PLS AC tartipores can also be seen in published PLS scans from at least six species of *Gelanor* which is the sister-lineage to all other mimetids, including *Australomimetes* (Platnick and Shadab 1993, Benavides and Hormiga 2016, Benavides et al. 2016). They are also present in many members of related spider families such as Tetragnathidae (Hormiga et al. 1995, Yoshida 1999, Álvarez-Padilla 2007, Álvarez-Padilla and Hormiga 2011) and Arkyidae (Platnick and Shadab 1993). Indeed, on the phylogenies presented in Wheeler et al. (2016) and Griswold and Ramírez (2017), PLS T-A AC are distributed, with losses, over a clade (CY spigot clade) that includes all araneomorphs except the Synspermiata, Filistatidae, and Hypochilidae (Platnick et al. 1991, Griswold et al. 2005, Ramírez 2014). Hence this character is symplesiomorphic for the family Mimetidae, with frequent losses in some genera and species being a secondary trait. Why the character has been lost independently many times within the family is unclear and further study is needed to clarify what adaptive reasons might account for the loss. The presence of PLS T-A AC in *Mimetes* and *Phobetinus*, but not *Ero* or (up to now) *Australomimetes*, was one of the characters indicating especially close affinity between *Phobetinus* and *Mimetes* (Townley et al. 2013). Our observations on *A. spinosus* now make this distinction less sharp. In all previously studied mimetids, if PLS AC tartipores were present, the basic arrangement on the PLS was for the non-T-A AC spigots to form a column roughly parallel to the long axis of the PLS, with all T-A AC spigots posterior to this column. *A. spinosus* is thus far unique, not only in being the only *Australomimetes* species found with T-A AC, but in being the only mimetid with T-A AC spigots forming two groups on each PLS, posterior and anterior to the non-T-A AC spigot column (Fig. 2B). Again, considering that PLS T-A AC occur in several mimetid genera and are widespread among araneomorphs, this character may have relatively little phylogenetic sig-

nal and ecology/biology of the species may account for the differences observed, with follow-up studies needed to clarify why some species have this trait and others do not.

Another variable character among different species of *Australomimetes* is the presence or absence of 2° MiA, as revealed by the presence/absence of a 2° MiA tartipore and either a 2° MiA spigot (juveniles) or an ontogenetic 2° MiA nubbin (adults) on each PMS. Previously, only one of the five aforementioned *Australomimetes* species was found to lack 2° MiA: *A. tasmaniensis*. This study clearly places *A. spinosus* in the larger contingent possessing 2° MiA (Figs 6A–D, 7), while *A. djuka* is now the second species known without 2° MiA (Figs 6E–H, 8) and thus unable to draw MiA silk during proecdysis. It is noteworthy that the two species, *A. tasmaniensis* and *A. djuka*, constitute the *tasmaniensis*-group in the cladistic analysis of Harms and Harvey (2009b), sister to all other *Australomimetes* species included in that analysis. Possession of 2° MiA has been considered the plesiomorphic condition for araneoids on phylogenetic grounds (Forster et al. 1990, Scharff and Coddington 1997, Griswold et al. 1998), which remains valid despite substantial changes proposed in higher-level spider phylogeny in recent years (Bond et al. 2014, Fernández et al. 2014, Dimitrov et al. 2016, Garrison et al. 2016, Wheeler et al. 2016). The consistent occurrence of an apparent phylogenetic 2° MiA nubbin on the PMS of 1<sup>st</sup> instars of *A. djuka* corroborates this view, clearly indicating the absence of 2° MiA in this species represents a secondary loss. This nubbin was located precisely where a 2° MiA spigot occurs in species that have 2° MiA (cf. Fig. 6A, E). Presumably, secondary loss also explains the absence of 2° MiA in five of seven examined *Ero* species (Platnick and Shadab 1993, Townley and Tillinghast 2009), whereas all examined species of *Mimetes*, *Phobetinus*, *Anansi*, and, most notably, the basal mimetid genus *Gelanor* have retained 2° MiA (Platnick and Shadab 1993, Griswold et al. 2005, Townley and Tillinghast 2009, Townley et al. 2013, Benavides and Hormiga 2016, Benavides et al. 2016).

Differences among species of *Australomimetes* with respect to these two characters, PLS T-A AC and 2° MiA, suggest that some species have greater silk needs during proecdysis, and ecdysis (Dolejš et al. 2014), than others, but it remains to be determined why this might be so.

### Constancy in the number of non-tartipore-accommodated (non-T-A) piriform silk glands (PI)

Figures 3–5 document increases in numbers of PI spigots during the ontogenies of *A. spinosus* and *A. djuka*. As observed in *Mimetes* and the araneid *Araneus* (Townley and Tillinghast 2009), these increases likely consisted solely of additional T-A PI spigots. The number of non-T-A PI spigots appeared to remain constant at two per ALS throughout development, starting from the 1<sup>st</sup> stadium. In part, the evidence for constancy in non-T-A PI number came from the pooled PI data in Table 2, though admittedly, because of intra-stadium variation in numbers of T-A PI spigots, comparing mean PI spigot counts at

one stadium with PI tartipore counts at the next stadium did not provide unequivocal evidence of such constancy. However, for those comparisons where there was no variation (1<sup>st</sup> to 2<sup>nd</sup> stadia in both species) or where we had larger numbers of observations (2<sup>nd</sup> to 3<sup>rd</sup> stadia and 3<sup>rd</sup> to 4<sup>th</sup> stadia in *A. spinosus*), a constant two non-T-A PI spigots/ALS was indicated.

Further evidence came from a 4<sup>th</sup> instar male *A. spinosus* that was well into proecdysis when it was preserved [see Results (Convention 5 in ‘Conventions applied...’)], allowing us to examine spinnerets on both the old (4<sup>th</sup> instar) and newly developed (pharate 5<sup>th</sup> instar) exoskeletons. This specimen was the source of all colorized images in Figs 4, 7, and 10. As demonstrated in earlier studies (Townley and Tillinghast 2009, Dolejš et al. 2014), comparing the same spinnerets in the same individual over two or more consecutive stadia is the most reliable way to distinguish T-A and non-T-A silk glands. Matching PI spigots on the old exoskeleton (Fig. 4A) with PI tartipores on the new exoskeleton (Fig. 4B) confirmed that all but two PI emptying on the right ALS were T-A during proecdysis in the 4<sup>th</sup> stadium. Blue T-A PI spigots in Fig. 4A correspond to blue PI tartipores in Fig. 4B; red PI spigots in Fig. 4A, B serve the two non-T-A PI associated with this ALS. The consistent positions occupied by the two non-T-A PI spigots were essentially the same as previously observed in *Mimetus* and *Araneus* (Townley and Tillinghast 2009: figs 5, 7).

To date, a pair of non-T-A PI associated with each ALS have only been indicated in three araneoid genera: *Araneus*, *Mimetus*, and now *Australomimetus*. In contrast, in the lycosids that have so far been examined, all PI are T-A (Dolejš et al. 2014, data for two consecutive stadia in one female *Pardosa* also noted in Townley and Tillinghast 2009: 376).

### Recurrent use of piriform and aciniform silk glands (PI, AC)

Dissections of cribellate orb-web builders, especially *Araneus*, at various points in the molt-intermolt cycle, have demonstrated that 1° ampullate silk glands (1° MaA and 1° MiA), being non-T-A, are re-used during each successive stadium (Townley et al. 1991, 1993, Townley 1993). 2° Ampullate silk glands (2° MaA and 2° MiA), being T-A, are also re-used, but only during alternating stadia; i.e., either during even-numbered stadia for one pair each of 2° MaA and 2° MiA, or during odd-numbered stadia for the other single pairs of 2° MaA and 2° MiA. Both 1° and 2° ampullate silk glands undergo dramatic re-modeling synchronized to the molt-intermolt cycle.

Because ampullate silk glands are relatively large, and few and constant in number across juvenile stadia, gross morphological changes can be monitored by dissection over the molt-intermolt cycle. PI and AC, on the other hand, generally occur as morphological multiples (Coddington 1989) and tend to be smaller, more numerous silk glands (e.g., Kokociński 1968, Mikulska 1969,

Wąsowska 1973, Mikulska and Wiśniewski 1979), less amenable to such individual monitoring by dissection. This, and the increases in AC and T-A PI numbers that occur during development, made it unclear whether individual AC and PI are also used during multiple stadia or only one (Townley and Tillinghast 2009). After all, given that some new PI and AC are added with most molts, might it be that the entire complement of PI and/or AC used during a given stadium (at least the T-A ones) is new and each of these silk glands functions only during one stadium? External observations made on spinnerets to date suggest the answer is no. Instead, like ampullate silk glands, once formed and functional, non-T-A AC/PI appear to function during every subsequent stadium while T-A AC/PI function during every other subsequent stadium. Dolejš et al. (2014), studying spiders of the family Lycosidae, provided persuasive evidence that relative arrangements of spigots/tartipores serving older PI/AC are to a large extent maintained during ontogeny and may, in many instances, be discerned at later stadia, this despite spigots serving newer PI and AC being added with each molt. The same conservation in positions of older PI and AC spigots/tartipores over multiple stadia was also indicated in the current study. In the proecdysial 4<sup>th</sup> instar *A. spinosus*, PI tartipores on the old exoskeleton in Fig. 4A (yellow) indicated the approximate arrangement of T-A PI spigots that must have existed on the right ALS during the 3<sup>rd</sup> stadium. The T-A PI spigots on the new exoskeleton of the pharate 5<sup>th</sup> instar in Fig. 4B included a group (yellow) in essentially the same arrangement. This apparently conserved PI spigot arrangement during the 3<sup>rd</sup> and (upcoming) 5<sup>th</sup> stadia suggests that the same individual T-A PI that functioned during the 3<sup>rd</sup> stadium were about to function again during the 5<sup>th</sup> stadium. T-A PI spigot complements at the 3<sup>rd</sup> and 5<sup>th</sup> stadia thereby differed only in that the latter also included a group of T-A PI that would have functioned for the first, and last, time during the 5<sup>th</sup> stadium (Fig. 4B, green): last only because this male would not have had a 7<sup>th</sup> stadium; adulthood would have been attained in the 6<sup>th</sup>. The consistent positions (relative to T-A PI spigots/tartipores) of the pair of non-T-A PI spigots on the old and new exoskeletons (Fig. 4A, B, red) indicated that the same individual non-T-A PI that functioned during the 4<sup>th</sup> stadium would have functioned again during the 5<sup>th</sup> stadium. Note that this pair of non-T-A PI spigots on each ALS are examples of PI spigots that are morphological singulars since each spigot of the pair can be individually specified: e.g., the anterior non-T-A PI spigot (Coddington 1989).

In the lycosids they studied, Dolejš et al. (2014) noted that new PI/AC spigots tended to be added centrifugally, at the periphery of spinning fields. This is likewise evident in Fig. 4B, where the new PI spigots (green) encircle spigots of the older PI (yellow) that had functioned during the 3<sup>rd</sup> stadium. We therefore anticipate that, internally, when new PI corpora form, it is at the periphery of the cluster of older PI corpora.

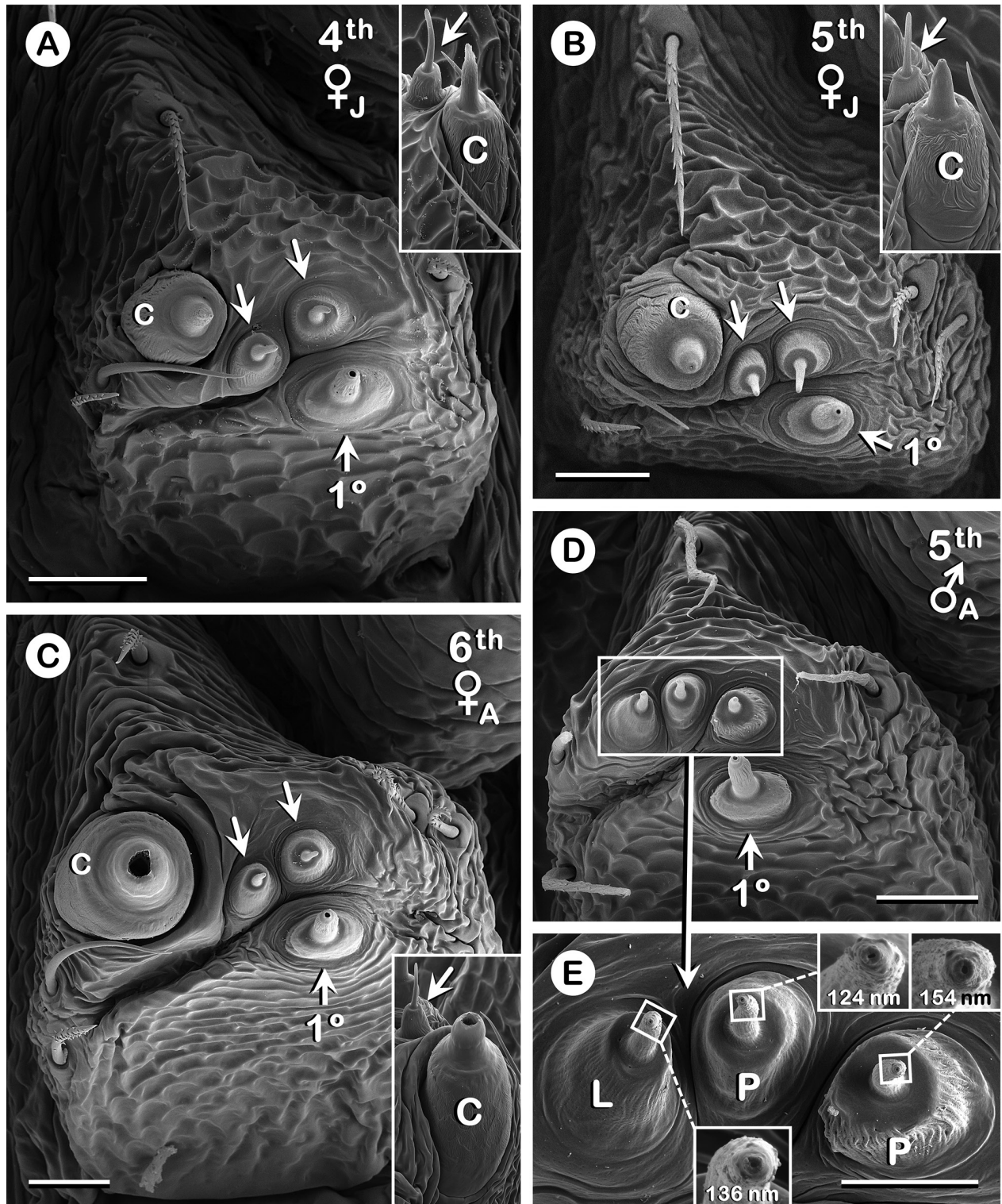


**Figure 8.** PMS of 4<sup>th</sup> to 6<sup>th</sup> instars of *Australomimetes djuka*. All unlabeled arrows point to non-T-A AC spigots. **A, B.** Juveniles. **C, D.** Adults. Same CY spigot (C) and closest AC spigot (unlabeled arrow) shown from two perspectives in (A, C); inset in (B) likewise from same specimen used to produce larger image, but shows lateral view of CY and AC spigots from opposite PMS. Note ontogenetic changes in CY spigot width relative to nearest AC spigot. **E.** AC spigots from (D) magnified, the distal ends of their shafts further magnified in insets: no obvious difference in diameters of openings, given in nm [see Materials and methods ('SEM of spinnerets...')], between 'late' AC spigot (L) and 'pioneer' AC spigots (P) [see Results ('PMS-Sexual and geographic...')]. **A, B inset, C.** Left PMS. **B main, D, E.** Right PMS (image flipped). 1°, 1° MiA spigot; C, CY spigot; L, 'late' AC spigot; P, 'pioneer' AC spigot. Scale bars: A-D 20  $\mu$ m; E 10  $\mu$ m. See also Abbreviations and terminology ('Spinning apparatus abbreviations') and Results (Convention 3 in 'Conventions applied...').

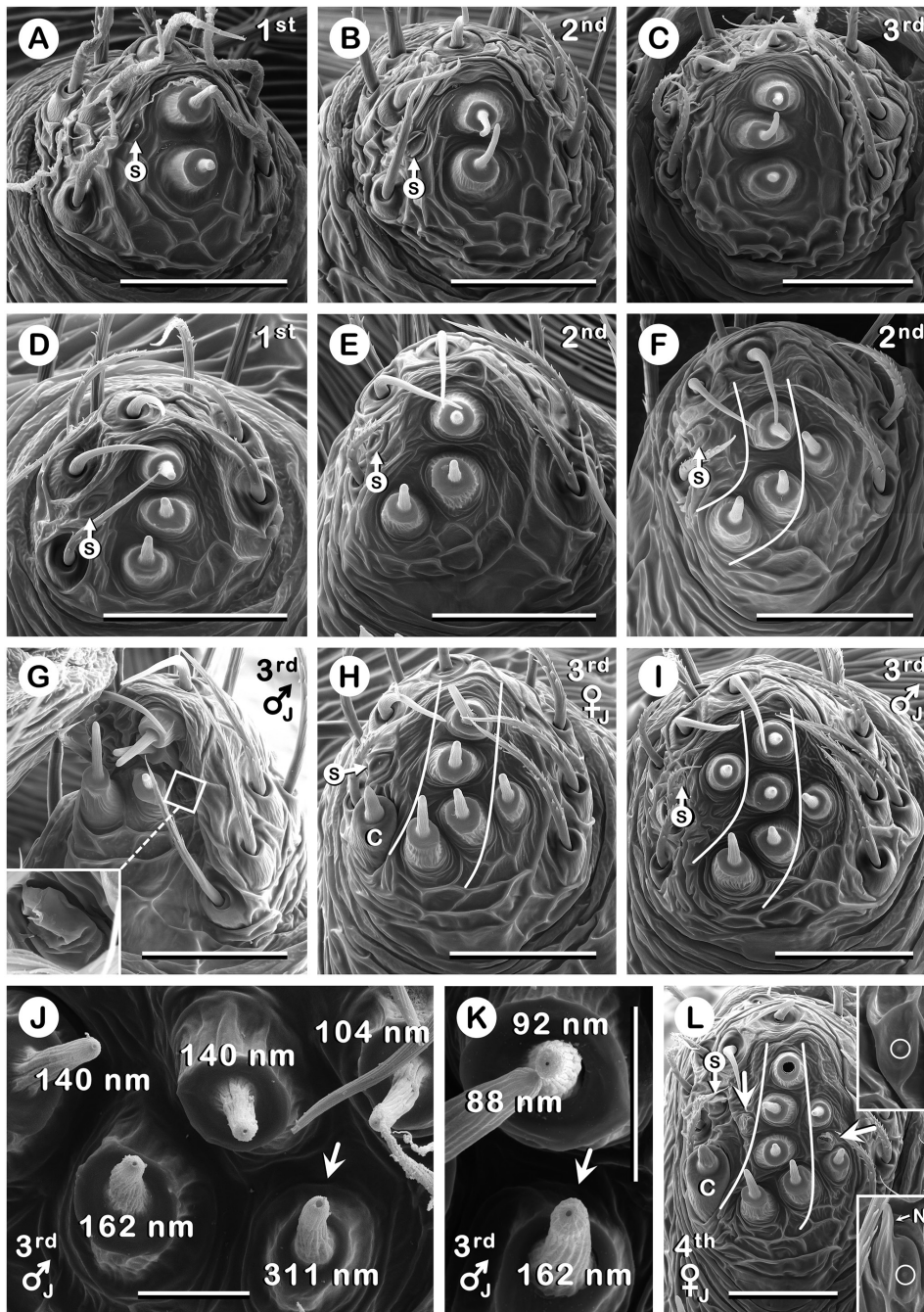


**Figure 9.** PLS of 1<sup>st</sup> to 3<sup>rd</sup> instars of *Australomimetus djuka* and 1<sup>st</sup> to 4<sup>th</sup> instars of *Australomimetus spinosus*. **A–C.** *A. djuka*. **D–L.** *A. spinosus*. All spigots in (**A–E**, **G**) are non-T-AAC spigots. AC spigots between two white curves in (**F**, **H**, **I**, **L**) are non-T-A; remainder are T-A. **E**, **F**. AC spigot complements in 2<sup>nd</sup> instars of *A. spinosus*: three non-T-A (**E**) (88%,  $N = 26$  PLS); three non-T-A, one posterior T-A (**F**) (12%). **G–I**. AC spigot complements in 3<sup>rd</sup> instars of *A. spinosus*: four non-T-A (**G**) (13%,  $N = 30$  PLS); four non-T-A, one posterior T-A (**H**) (63%); four non-T-A, one anterior T-A (not shown) (3%); four non-T-A, one posterior T-A, one anterior T-A (**I**) (20%). One posterior AC tartipore (**G**, magnified in inset) observed in 7% of 3<sup>rd</sup> stadium PLS; the rest had none. **H**. CY spigots (**C**) first appeared in 3<sup>rd</sup> instars of *A. spinosus*. **J**, **K**. AC spigots on PLS from different *A. spinosus* specimens, showing larger diameter openings on T-A AC spigots (arrows) compared with neighboring non-T-A AC spigots [see Results ('PLS')]; measurements given in nm [see Materials and methods ('SEM of spinnerets...')]. **L**. PLS containing possible phylogenetic nubbin, adjacent to putative sensillum (**S**), in position consistent with araneoid AG-FL spigots. Lower inset, same nubbin (**N**) and sensillum magnified, anterior view; upper inset, sensillum from opposite PLS, lacking a nubbin; circles indicate (indistinct) raised-rim pores that are part of sensilla. More distinct pores can be seen in Townley and Tillinghast (2009) figs 8I, 9D, 13K, 20B, 22C and Townley et al. (2013) figs 2G, 4G. Unlabeled arrows point to AC tartipores, one anterior, one posterior, indicating an AC spigot arrangement during preceding (3<sup>rd</sup>) stadium like that shown in (**I**). **D**, **E**, **G**, **I–K**, **L** upper inset. Left PLS. **A–C**, **F**, **H**, **L** main, **L** lower inset. Right PLS (image flipped). **C**, CY spigot; **S**, putative sensillum. Scale bars: **A–I**, **L** 20  $\mu\text{m}$ ; **J**, **K** 5  $\mu\text{m}$ . See also Abbreviations and terminology ('Spinning apparatus abbreviations') and Results (Convention 3 in 'Conventions applied...').

In *A. spinosus*, conserved arrangements of AC spigots on the PLS during development largely mirrored those of PI spigots on the ALS. Thus, AC tartipores on the old exoskeleton in Fig. 10A, B (yellow) indicated the positions taken by T-A AC spigots during the preceding 3<sup>rd</sup> stadium. In the pharate 5<sup>th</sup> instar, T-A AC spigots (yellow) again occupied these positions (Fig. 10C, D, respectively), indicating that the same T-A AC that functioned during the 3<sup>rd</sup> stadium would have returned to use during the 5<sup>th</sup> stadium. Along with these returning T-A AC, PLS during the 5<sup>th</sup> stadium would have had three (Fig. 10C, green) or two (Fig. 10D, green) new T-A AC available for use as well. One departure from the ALS PI condition concerned the non-T-A AC associated with the PLS (Fig. 10A–D, red + fuchsia) since their number was not constant from stadium to stadium, as it was for the two non-T-A PI (Fig. 4A, B, red). Instead, from the 2<sup>nd</sup> stadium forward, the number of non-T-A AC increased by one on each PLS from one stadium to the next (Table 3), the spigot serving the new non-T-A AC added to the distal end of the non-T-A AC spigot column (Fig. 10C, D, fuchsia).

Though a given T-A AC or PI functions only during alternate stadia, there are indications, particularly from the PLS T-A AC in *A. spinosus*, that these silk glands have some latitude with respect to when they “enter the work force”. That is, an individually specifiable T-A AC may function during odd-numbered stadia in some specimens, but function during even-numbered stadia in other specimens. Consider the following: most (88%,  $N = 26$  PLS) 2<sup>nd</sup> stadium PLS had no T-A AC spigots (Fig. 9E), but a minority (12%) had one posterior T-A AC spigot (Fig. 9F). This one T-A AC was responsible for an AC tartipore in the expected location (Fig. 9G), also in a minority (7%,  $N = 30$  PLS) of 3<sup>rd</sup> stadium PLS. These PLS with one AC tartipore had no T-A AC spigots even though most (87%) 3<sup>rd</sup> stadium PLS had one (Fig. 9H) or two (Fig. 9I) T-A AC spigots, but no AC tartipores. This suggests that the single posterior T-A AC spigot seen in Figs 9F and 9H, consistently located, represents the same individually specifiable AC, sometimes functional from the 2<sup>nd</sup> stadium and then again during later even-numbered stadia, but more often functional from the 3<sup>rd</sup> stadium and then again during later odd-numbered stadia. If it functions, one might say prematurely, during the 2<sup>nd</sup> stadium, it is not available for use during the 3<sup>rd</sup> stadium, with the result that 3<sup>rd</sup> stadium PLS with an AC tartipore tend to not have T-A AC spigots, while those without an AC tartipore tend to have at least one T-A AC spigot.

### Modified piriform silk glands (MoPI) in adult male mimetids

Adult males of *A. spinosus* and *A. djuka* did not exhibit a pair of spigots on each ALS serving modified PI (MoPI). Such spigots, located near the 2<sup>o</sup> MaA tartipore, have been found exclusively in adult males of some mimetid species. They are conspicuously different from other PI spigots, with wider shafts and openings, and segregated

from the other PI spigots. It is unknown what purpose MoPI serve, but their restriction to adult males advocates for investigation of silken structures specific to courtship and mating (Bristowe 1958). The most parsimonious hypothesis regarding MoPI origin is that they are simply the pair of non-T-A PI associated with each ALS [see Discussion (‘Constancy in the number...’)], in use since the first stadium, but more dramatically transformed during their final proecdysial re-modeling (Townley and Tillinghast 2009, Townley et al. 2013). We cannot say with certainty that MoPI are transformed non-T-A PI because, in those mimetids in which MoPI form, we have not been certain that more typical non-T-A PI are not present concurrently. In part, this is because definitive proof of T-A or non-T-A status during one stadium resides in the exoskeleton from the next stadium, and for adults there is no next stadium. Also, because of ontogenetic increases in numbers of T-A PI, attempts to use conserved PI spigot/tartipore arrangements from earlier stadia [noted in Discussion (‘Recurrent use...’)] to make this determination have so far produced ambiguous results.

MoPI spigots were first described in two North American and one South American species of *Mimetus* (Townley and Tillinghast 2009, see also Townley et al. 2013: fig. 1B–D), and apparent in a third North American species (Griswold et al. 2005: fig. 26B). Townley and Tillinghast (2009) suggested they may be a synapomorphy for *Mimetus*. This was initially refuted when they were subsequently observed in adult males of the type species of *Phobetinus* (Townley et al. 2013). However, one consequence of the phylogenetic analyses of Benavides and Hormiga will be that *Phobetinus* becomes a junior synonym of *Mimetus* (Benavides et al. 2016). The possibility that MoPI spigots may be a synapomorphy for a delimited *Mimetus* that, among other changes (Benavides et al. 2016), incorporates *Phobetinus* (Townley et al. 2013) was also refuted when they were later observed in the most basal mimetid genus *Gelanor* (adult males of three species, Benavides and Hormiga 2016). Thus, MoPI spigots may be a synapomorphy for the entire family Mimetidae, again with secondary losses having occurred in individual species or even genera.

MoPI spigots like those in *Mimetus*, *Phobetinus*, and *Gelanor* have not been evident in those *Ero* or *Australomimetus* species examined to date (Harms and Harvey 2009b, Townley and Tillinghast 2009). However, adult males of two of five examined *Ero* species have been found with what have been referred to as ‘subtle MoPI spigots’, with modestly wider openings than other PI spigots, but not substantially wider shafts and not set apart from other PI spigots (Townley and Tillinghast 2009). Like MoPI and non-T-A PI spigots, they number two per ALS. Subtle MoPI spigots were not found in *A. auriculatus*, *A. diabolicus*, or *A. tasmaniensis* (Townley and Tillinghast 2009), but Townley et al. (2013) noted their presence in *A. sydneyensis*. The morphology and positions of subtle MoPI spigots are so similar to those of non-T-A PI spigots that a non-T-A PI origin for subtle MoPI seems inescap-

able. This, in turn, supports a non-T-A PI origin for MoPI as well, with subtle MoPI seemingly exhibiting a degree of transformation during the last proecdysis intermediate between the high extreme of MoPI and the low extreme of typical non-T-A PI. Presumably, internal investigations of the PI will make MoPI and subtle MoPI origins clear. In any case, *A. sydneyensis* is currently unique among *Australomimetus*, since *A. spinosus* and *A. djuka* did not exhibit even subtle MoPI spigots in adult males (Figs 4D, E, 5B, C).

### Cylindrical silk gland (CY) spigots

CY, also known as tubuliform silk glands, are used by adult females in the construction of egg sacs. The two *Australomimetus* species examined in this study exhibited the unusually large, wide-aperture CY spigots typical of adult female mimetines (Platnick and Shadab 1993), one per PMS and PLS, unlike the two per PLS that are present in gelanorines (Platnick and Shadab 1993, Benavides and Hormiga 2016) and considered plesiomorphic for araneoids (Griswold et al. 1998). CY spigots were also present in juvenile females, as early as the 3<sup>rd</sup> stadium in *A. spinosus*, which agrees with findings in two *Mimetus* species (Townley and Tillinghast 2009). We are not, however, aware of any evidence that they are used in juveniles. To the contrary, histological observations indicate that, at least in general, CY become functional only in adults concurrent with vitellogenesis in the ovaries (Richter 1970, Kovoor 1977, 1987). If juvenile mimetine CY were to produce silk fibers, they would presumably be much thinner than those drawn from adult CY spigots since juvenile CY spigots lack the wide shafts and openings of adults. It was observed in *A. spinosus* that the full complement of four CY spigots was not present in a large majority of 3<sup>rd</sup> stadium females. Similarly, in *Araneus cavaticus*, CY spigots first appear in 4<sup>th</sup> stadium females, but often not with the full complement of six spigots present during later stadia (Townley and Tillinghast 2009). Müller and Westheide (1993) hypothesized that the presence of CY spigots in juveniles indicates that their female ancestors matured at earlier stadia. If true, this would suggest that female ancestors of *Australomimetus* matured as early as the 3<sup>rd</sup> stadium, which is at least a possibility among small spiders (Gertsch 1979).

The deep incising typical of CY spigot shafts in *Ero* and *Mimetus* (Platnick and Shadab 1993, Schütt 2000, Griswold et al. 2005, Townley and Tillinghast 2009, Townley et al. 2013), but not *Phobetinus* (Townley et al. 2013) or previously examined *Australomimetus* (Harms and Harvey 2009a, b, Townley and Tillinghast 2009), was also not evident in *A. spinosus* or *A. djuka*. There were, however, more minor differences between CY spigot shafts in the two species, including shallow incising in *A. spinosus* that was lacking in *A. djuka* [see Results ('Cylindrical silk gland...')].

Remarkably, though the newly described mimetid genus *Anansi* nests within the subfamily Mimetinae, scans

of their spinnerets (Benavides et al. 2016) demonstrate that adult females have more conventional CY spigots and not the enlarged, rotund, wide-aperture CY spigots of most mimetines. Moreover, while at least one species has a single CY spigot on each PLS, typical of mimetines, at least two other species have no CY spigot on the PLS (Benavides et al. 2016). The latter retain only the single CY spigot on each PMS [fig. 17G in Benavides et al. (2016) has two spigots on a PMS labeled CY, but the lower one, given its position near the 2° MiA nubbin and tartipore, is presumably the 1° MiA spigot despite its morphology being similar to the authentic CY spigot]. These departures from the typical mimetine condition may be attributable to maternal care behavior observed in the genus (Benavides et al. 2016). Females carry eggs and postembryos with their chelicerae, and photos of this behavior indicate minimal wrapping with silk. This contrasts with the substantial egg sacs of most other mimetines (Guarisco and Mott 1990, Guarisco 2001, Thaler et al. 2004, Harms and Harvey 2009b, Kúrka et al. 2015, Killick 2016) and lack of maternal care (Bristowe 1958). Benavides et al. (2016) also observed maternal care and apparently insubstantial egg sacs in two neotropical mimetines currently placed in *Mimetus*. It will be of interest to determine the status of their CY spigots.

### Aciniform silk gland (AC) spigot numbers in *A. spinosus*: sexual and geographic dimorphisms

With the exception of a single PMS, there were two AC spigots on each PMS in four adult female *A. spinosus*. In contrast, five adult males had 3–5 AC spigots on each PMS and one juvenile male from eastern Australia had three per PMS (Table 3). Published data for *A. aurioculatus* indicate that essentially the same sexual dimorphism also applies to that species (Townley et al. 2013, see fig. 18G, H in Townley and Tillinghast 2009). Two adult female *A. aurioculatus* had two AC spigots per PMS while two adult males had 4–6 AC spigots per PMS. The additional ('late') AC spigots in males, with wider apertures than the two 'pioneer' AC spigots (Fig. 7D–G), extended toward the area occupied by CY spigots in females, raising the possibility that this dimorphism may be attributable to space constraints. It is true, however, that large CY spigots have not prevented some adult female mimetines (North American *Mimetus* species) from fitting four AC spigots per PMS (Griswold et al. 2005: fig. 25C, Townley and Tillinghast 2009: fig. 17B). Our very limited data from *A. djuka* indicate a less distinct difference in PMS AC spigot number between the sexes.

The specimens of *A. spinosus* examined in this study included examples from Western Australia and from the eastern states of Queensland and New South Wales. Only slight differences in spinneret features were indicated between these populations, and because of the limited data, additional observations will be required to verify or refute them. These differences concerned the (never high) numbers of AC spigots, with eastern specimens tending



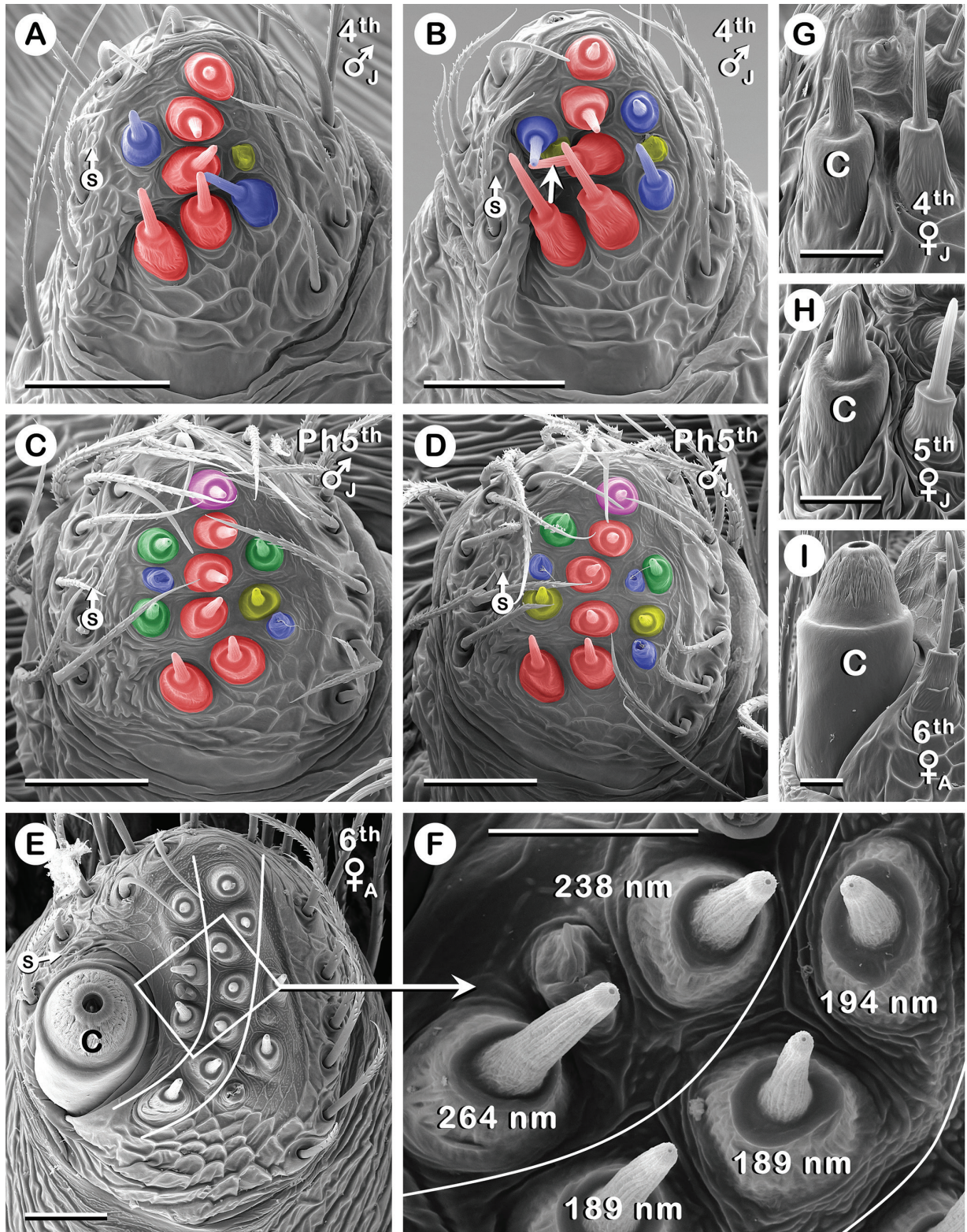


**Figure 10.** PLS of 4<sup>th</sup> to 6<sup>th</sup> instars of *Australomimetus spinosus*. A–D. PLS from one juvenile specimen, well into proecdysis. Color coding explained in Results (Convention 5 in ‘Conventions applied...’). A, B. Old exoskeleton. C, D. New exoskeleton directly beneath (A, B), respectively. One of two AC tartipores (yellow) in (B) largely obscured (unlabeled arrow). E, F. Adult, AC spigots between two white curves are non-T-A; the rest, anterior and posterior, are T-A. AC spigots in boxed region of (E) magnified in (F), showing larger diameter openings in T-A AC spigots compared with neighboring non-T-A AC spigots [see Results (‘PLS’)]; measurements given in nm [see Materials and methods (‘SEM of spinnerets...’)]. G–I. Ontogenetic changes in CY spigot (C) morphology; medial, high tilt view. Note changes in width relative to AC spigot on right. (E, F, I) all from same PLS. B, D–F, I. Left PLS. A, C, G, H. Right PLS (image flipped). C, CY spigot; S, putative sensillum. Scale bars: A–E 20  $\mu$ m; F–I 10  $\mu$ m. See also Abbreviations and terminology (‘Spinning apparatus abbreviations’) and Results (Convention 3 in ‘Conventions applied...’).

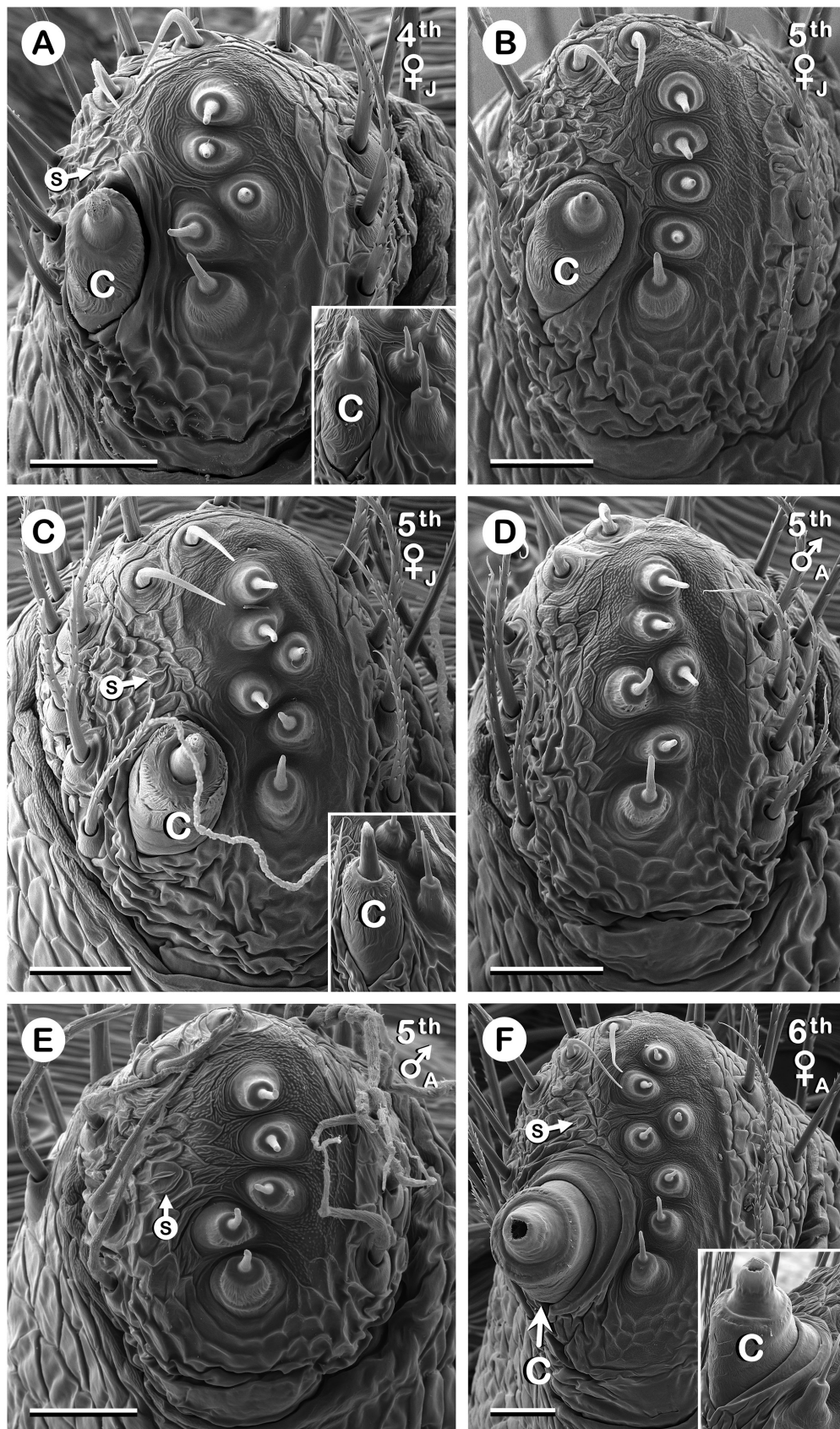


**Figure 11.** PLS of 4<sup>th</sup> to 6<sup>th</sup> instars of *Australomimetes djuka*. All spigots other than CY spigots (C) are non-T-A AC spigots. A–C. Juveniles. D–F. Adults. B–E. Unlike *A. spinosus*, variation observed in non-T-A AC spigot number within same stadium and state of maturity. CY spigot and nearby AC spigots shown from two perspectives in (A, C, F). B, C, E, F. Left PLS. A, D. Right PLS (image flipped). C, CY spigot; S, putative sensillum. All scale bars 20  $\mu$ m. See also Abbreviations and terminology (‘Spinning apparatus abbreviations’) and Results (Convention 3 in ‘Conventions applied...’).

to have more T-A AC spigots on PLS and, among older males, more non-T-A AC spigots on PMS (Table 3). There is recent genetic evidence that Western Australian *A. spinosus* populations are sufficiently distinct from eastern populations to define them as a separate species (Harms in prep.), but the morphology of the genitalia in both sexes is cryptic and additional studies of spigot structure may offer a possibility to delineate both candidate species on morphological grounds. Ecology certainly suggests a split into distinct species because the WA populations of *A. spinosus* occur on rocky outcrops whereas the eastern populations are from subtropical rainforest habitats and the observed AC differences, if consistent, may reflect ecologically-driven genetic divergence.

### Ampullate silk gland tartipore primordia in 1<sup>st</sup> instars

In most, if not all, araneomorphs, functional T-A silk glands are first available for use in 1<sup>st</sup> instars (Townley and Tillinghast 2003, Dolejš et al. 2014). Consequently, tartipores first form and function in the exoskeleton of the pharate 2<sup>nd</sup> instar, during proecdysis of the 1<sup>st</sup> stadium [see Abbreviations and terminology ('Terminology'), Fig. 1], and are therefore not observable externally until the 2<sup>nd</sup> stadium. In 1<sup>st</sup> instars of *A. spinosus* and *A. djuka*, a round/oval structure was seen lateral to the 2° MaA spigot on each ALS (Fig. 3A, D), near the location taken by a 2° MaA tartipore beginning in pharate 2<sup>nd</sup> instars. A comparable structure was observed adjacent to the 2° MiA spigot on each PMS, but only in *A. spinosus* (Fig. 6A). Such structures have been noted before, on 1<sup>st</sup> instars of lycosids, gnaphosids, uloborids, araneids, and mimetids (*Mimetus*) (Townley and Tillinghast 2003, 2009), and presumed to be ampullate silk gland tartipore primordia (called pre-tartipores in the 2003 paper) given their locations and restriction to 1<sup>st</sup> instars. It is consistent with this identification that *A. djuka*, a species that lacked 2° MiA tartipores at all stadia (Figs 6G, H, 8), showed no sign of these putative primordia on PMS of 1<sup>st</sup> instars (Fig. 6E, F).

The position taken by the structure in question on PMS of 1<sup>st</sup> instars of *A. spinosus* was also consistent with a tartipore primordium identity. Relative to the 2° MiA spigot, its location varied over about a 90° arc on different 1<sup>st</sup> stadium PMS, from directly anterior to the spigot (as in Fig. 6A) to directly lateral to the spigot. In 2<sup>nd</sup> and later instars, the 2° MiA tartipore and spigot (or nubbin, in adults) switched positions from one stadium to the next (Figs 6B–D, 7A–D, F), such that the tartipore was posteromedial to the spigot in even-numbered instars and anterolateral to the spigot in odd-numbered instars (Table 2). Thus, a 2° MiA tartipore primordium would be expected in the anterolateral position in 1<sup>st</sup> instars. The anterior-to-lateral position that was observed fits this prediction well.

### Phylogenetic aggregate-flagelliform silk gland (AG-FL) triad nubbin

Like other Mimetidae (Platnick and Shadab 1993, Schütt 2000, Griswold et al. 2005, Townley et al. 2013, Mur-

phy and Roberts 2015, Benavides and Hormiga 2016), including other species of *Australomimetus* (Harms and Harvey 2009a, b, Townley and Tillinghast 2009), the two species studied here lacked spigots of AG and FL on the PLS. As these two silk gland types are synapomorphic for Araneoidea (Coddington 1986, Griswold et al. 1998, Schütt 2000, 2003), these absences presumably represent secondary losses associated with araneophagy and abandonment of capture-web construction (Platnick and Shadab 1993, Schütt 2000). However, it may be that vestiges of these silk glands remain in the form of occasional phylogenetic nubbins and associated sensilla. In a SEM study of 156 PLS from 1<sup>st</sup> to 6<sup>th</sup> instars of *Mimetus*, nine (6%) had a cuticular protuberance in a location consistent with an araneoid AG-FL triad (three spigots: two AG, one FL) (Townley and Tillinghast 2009). These protuberances were tentatively identified as phylogenetic nubbins, possibly of AG or FL spigots, a suggestion consistent with a growing consensus that mimetids are closely related to the araneoid family Tetragnathidae (Blackledge et al. 2009, Dimitrov and Hormiga 2011, Dimitrov et al. 2012, Bond et al. 2014, Hormiga and Griswold 2014, Benavides et al. 2016, Dimitrov et al. 2016, Garrison et al. 2016, Wheeler et al. 2016). Putative sensilla associated with these nubbins and with AG/FL spigots in typical araneoids (several indicated in Figs 9–11), and similarities between these nubbins and those occasionally seen in the same location in the araneid *Cyrtophora*, have been discussed previously (Townley and Tillinghast 2009, Townley et al. 2013). In this study, a total of 148 PLS from 1<sup>st</sup> to 6<sup>th</sup> instars of *Australomimetus* were examined, and only one nubbin of this type was observed (0.7%) (Fig. 9L).

### Acknowledgements

We are immensely grateful to collectors of some of the specimens examined in this study: G.J. Anderson, C.J. Burwell, R. Foulds, R. Graham, M. Gray, S.M. Harms, M.S. Harvey, W.F. Humphreys, G. Milledge, A. Nakamura, J. Norman, J. Peck, S. Peck, C. Rippon, H. Smith, and J.M. Waldock. We are also thankful to M.S. Harvey and Julianne Waldock (Western Australian Museum), Robert Raven and Owen Seeman (Queensland Museum), and Graham Milledge (Australian Museum) for the loan of specimens from their collections, and to Petr Dolejš (National Museum-Natural History Museum, Praha) and an anonymous reviewer for many helpful comments that improved the manuscript. Stephanie Harms assisted with the collection of prey spiders for the hungry pack and raising several hundred pirate spider babies would have been impossible without her fierce efforts. Charlene Newton very generously assisted with the creation of Fig. 1 and Table 1. The Tescan SEM so critical to this study, housed within the University Instrumentation Center (UIC) at the University of New Hampshire, was acquired with funding provided in part by the U.S. National Science Foundation (Major Research Instrumentation grant 1337897) and is

managed with great kindness by Nancy Cherim (UIC). Many thanks to her and to Todd Gross (Mechanical Engineering and Materials Science, UNH), PI on the NSF grant proposal.

## References

- Álvarez-Padilla F (2007) Systematics of the spider genus *Metabus* O.P.-Cambridge, 1899 (Araneoidea: Tetragnathidae) with additions to the tetragnathid fauna of Chile and comments on the phylogeny of Tetragnathidae. *Zoological Journal of the Linnean Society* 151: 285–335. <https://doi.org/10.1111/j.1096-3642.2007.00304.x>
- Álvarez-Padilla F, Hormiga G (2011) Morphological and phylogenetic atlas of the orb-weaving spider family Tetragnathidae (Araneae: Araneoidea). *Zoological Journal of the Linnean Society* 162: 713–879. <https://doi.org/10.1111/j.1096-3642.2011.00692.x>
- Benavides LR, Hormiga G (2016) Taxonomic revision of the Neotropical pirate spiders of the genus *Gelanor* Thorell, 1869 (Araneae, Mimetidae) with the description of five new species. *Zootaxa* 4064: 1–72. <https://doi.org/10.11646/zootaxa.4064.1.1>
- Benavides LR, Giribet G, Hormiga G (2016) Molecular phylogenetic analysis of “pirate spiders” (Araneae, Mimetidae) with the description of a new African genus and the first report of maternal care in the family. *Cladistics* 33: 375–405. <https://doi.org/10.1111/cla.12174>
- Blackledge TA, Scharff N, Coddington JA, Szüts T, Wenzel JW, Hayashi CY, Agnarsson I (2009) Reconstructing web evolution and spider diversification in the molecular era. *Proceedings of the National Academy of Sciences of the United States of America* 106: 5229–5234. <https://doi.org/10.1073/pnas.0901377106>
- Blackledge TA, Kuntner M, Agnarsson I (2011) The form and function of spider orb webs: evolution from silk to ecosystems. *Advances in Insect Physiology* 41: 175–262. <https://doi.org/10.1016/B978-0-12-415919-8.00004-5>
- Bond JE, Garrison NL, Hamilton CA, Godwin RL, Hedin M, Agnarsson I (2014) Phylogenomics resolves a spider backbone phylogeny and rejects a prevailing paradigm for orb web evolution. *Current Biology* 24: 1765–1771. <https://doi.org/10.1016/j.cub.2014.06.034>
- Bristowe WS (1941) *The Comity of Spiders, Volume II*. Ray Society (Number 128), London, 560 pp.
- Bristowe WS (1958) *The World of Spiders*. Collins, London, 304 pp.
- Carlson RW (1983) Instar, stadium, and stage: definitions to fit usage. *Annals of the Entomological Society of America* 76: 319. <https://doi.org/10.1093/aesa/76.3.319>
- Coddington J (1986) The monophyletic origin of the orb web. In: Shear WA (Ed) *Spiders: Webs, Behavior, and Evolution*. Stanford University Press, Stanford, 319–363.
- Coddington JA (1989) Spinneret silk spigot morphology: evidence for the monophyly of orbweaving spiders, Cyrtophorinae (Araneidae), and the group Theridiidae plus Nesticidae. *Journal of Arachnology* 17: 71–95. <http://www.jstor.org/stable/3705406>
- Cormier Z (2017) BBC Earth: ‘Pirate spiders’ make a living by preying on other spiders. <http://www.bbc.com/earth/story/20170608-pirate-spiders-make-a-living-by-preying-on-other-spiders>
- Cutler B (1972) Notes on the biology of *Mimetus puritanus* Chamberlin (Araneae: Mimetidae). *American Midland Naturalist* 87: 554–555. <https://doi.org/10.2307/2423592>
- Czajka M (1963) Nieznane szczegóły z życia pająka *Ero furcata* (Villers) (Mimetidae, Araneae) [Unknown facts of the biology of the spider *Ero furcata* (Villers) (Mimetidae, Araneae)]. *Polskie Pismo Entomologiczne [Bulletin Entomologique de Pologne]* 33: 229–231.
- Dimitrov D, Hormiga G (2011) An extraordinary new genus of spiders from Western Australia with an expanded hypothesis on the phylogeny of Tetragnathidae (Araneae). *Zoological Journal of the Linnean Society* 161: 735–768. <https://doi.org/10.1111/j.1096-3642.2010.00662.x>
- Dimitrov D, Lopardo L, Giribet G, Arnedo MA, Álvarez-Padilla F, Hormiga G (2012) Tangled in a sparse spider web: single origin of orb weavers and their spinning work unravelled by denser taxonomic sampling. *Proceedings of the Royal Society B* 279: 1341–1350. <https://doi.org/10.1098/rspb.2011.2011>
- Dimitrov D, Benavides LR, Arnedo MA, Giribet G, Griswold CE, Scharff N, Hormiga G (2016) Rounding up the usual suspects: a standard target-gene approach for resolving the interfamilial phylogenetic relationships of cribellate orb-weaving spiders with a new family-rank classification (Araneae, Araneoidea). *Cladistics* 33: 221–250. <https://doi.org/10.1111/cla.12165>
- Dolejš P, Buchar J, Kubcová L, Smrž J (2014) Developmental changes in the spinning apparatus over the life cycle of wolf spiders (Araneae: Lycosidae). *Invertebrate Biology* 133: 281–297. <https://doi.org/10.1111/ivb.12055>
- Downes MF (1987) A proposal for standardization of the terms used to describe the early development of spiders, based on a study of *Theridion rufipes* Lucas (Araneae: Theridiidae). *Bulletin of the British Arachnological Society* 7: 187–193. <http://britishspiders.org.uk/members/bulletin/070609.pdf>
- Fernández R, Hormiga G, Giribet G (2014) Phylogenomic analysis of spiders reveals nonmonophyly of orb weavers. *Current Biology* 24: 1772–1777. <https://doi.org/10.1016/j.cub.2014.06.035>
- Forster RR, Platnick NI, Coddington J (1990) A proposal and review of the spider family Synotaxidae (Araneae, Araneoidea), with notes on theridiid interrelationships. *Bulletin of the American Museum of Natural History* 193: 1–116. <http://hdl.handle.net/2246/883>
- Garrison NL, Rodriguez J, Agnarsson I, Coddington JA, Griswold CE, Hamilton CA, Hedin M, Kocot KM, Ledford JM, Bond JE (2016) Spider phylogenomics: untangling the Spider Tree of Life. *PeerJ* 4:e1719. doi:10.7717/peerj.1719
- Gertsch WJ (1979) *American Spiders*. Second Edition. Van Nostrand Reinhold Co, New York, 274 pp.
- Griswold CE, Coddington JA, Hormiga G, Scharff N (1998) Phylogeny of the orb-web building spiders (Araneae, Orbiculariae: Deinopoidea, Araneoidea). *Zoological Journal of the Linnean Society* 123: 1–99. <https://doi.org/10.1111/j.1096-3642.1998.tb01290.x>
- Griswold CE, Ramirez MJ, Coddington JA, Platnick NI (2005) Atlas of phylogenetic data for entelegyne spiders (Araneae: Araneomorphae: Entelegynae) with comments on their phylogeny. *Proceedings of the California Academy of Sciences, 4th Series* 56 (Supplement II): 1–324.
- Griswold CE, Ramirez MJ (2017) Phylogeny of spiders. In: Ubick D, Paquin P, Cushing PE, Roth V (Eds) *Spiders of North America: an Identification Manual*. Second Edition. American Arachnological Society, Keene, New Hampshire, 17–29.
- Guarisco H (2001) Description of the egg sac of *Mimetus notius* (Araneae, Mimetidae) and a case of egg predation by *Phalacrotophora epeirae* (Diptera, Phoridae). *Journal of Arachnology* 29: 267–269. [https://doi.org/10.1636/0161-8202\(2001\)029\[0267:DOTESO\]2.0.CO;2](https://doi.org/10.1636/0161-8202(2001)029[0267:DOTESO]2.0.CO;2)

- Guarisco H, Mott DJ (1990) Status of the genus *Mimetus* (Araneae: Mimetidae) in Kansas and a description of the egg sac of *Mimetus puritanus* Chamberlin. *Transactions of the Kansas Academy of Science* 93: 79–84. <https://doi.org/10.2307/3628149>
- Harms D, Dunlop JA (2009) A revision of the fossil pirate spiders (Arachnida: Araneae: Mimetidae). *Palaeontology* 52: 779–802. <https://doi.org/10.1111/j.1475-4983.2009.00890.x>
- Harms D, Harvey MS (2009a). A review of the pirate spiders of Tasmania (Arachnida: Mimetidae: *Australomimetus*) with description of a new species. *Journal of Arachnology* 37: 188–205. <https://doi.org/10.1636/A08-35.1>
- Harms D, Harvey MS (2009b) Australian pirates: systematics and phylogeny of the Australasian pirate spiders (Araneae: Mimetidae), with a description of the Western Australian fauna. *Invertebrate Systematics* 23: 231–280. <https://doi.org/10.1071/IS08015>
- Hilbrant M, Damen WGM, McGregor AP (2012) Evolutionary crossroads in developmental biology: the spider *Parasteatoda tepidariorum*. *Development* 139: 2655–2662. <https://doi.org/10.1242/dev.078204>
- Hormiga G, Eberhard WG, Coddington JA (1995) Web-construction behavior in Australian *Phonognatha* and the phylogeny of nephiline and tetragnathid spiders (Araneae: Tetragnathidae). *Australian Journal of Zoology* 43: 313–364. <https://doi.org/10.1071/ZO9950313>
- Hormiga G, Griswold CE (2014) Systematics, phylogeny, and evolution of orb-weaving spiders. *Annual Review of Entomology* 59: 487–512. <https://doi.org/10.1146/annurev-ento-011613-162046>
- Jackson RR (1992) Eight-legged tricksters: Spiders that specialize in catching other spiders. *BioScience* 42: 590–598. <https://doi.org/10.2307/1311924>
- Jackson RR, Whitehouse MEA (1986) The biology of New Zealand and Queensland pirate spiders (Araneae, Mimetidae): aggressive mimicry, araneophagy and prey specialization. *Journal of Zoology, London Series A* 210: 279–303. <https://doi.org/10.1111/j.1469-7998.1986.tb03635.x>
- Jackson RR, Cross FR (2015) Mosquito-terminator spiders and the meaning of predatory specialization. *Journal of Arachnology* 43: 123–142. <https://doi.org/10.1636/V15-28>
- Killick T (2016) *Ero aphana* in a Gloucestershire garden. *Newsletter of the British Arachnological Society* 136: 12–13. <http://srs.britishtspiders.org.uk/resource/SRSNL85.pdf>
- Kloock CT (2001) Diet and insectivory in the “araneophagic” spider, *Mimetus notius* (Araneae: Mimetidae). *American Midland Naturalist* 146: 424–428. [https://doi.org/10.1674/0003-0031\(2001\)146\[0424:-DAIITA\]2.0.CO;2](https://doi.org/10.1674/0003-0031(2001)146[0424:-DAIITA]2.0.CO;2)
- Kloock CT (2012) Natural history of the pirate spider *Mimetus hesperus* (Araneae: Mimetidae) in Kern County, California. *Southwestern Naturalist* 57: 417–420. <https://doi.org/10.1894/0038-4909-57.4.417>
- Kokociński W (1968) Studia biometryczne nad wzrostem kądziółków przędnych w rozwoju postembrionalnym pająka *Agelena labyrinthica* (Clerck) (Araneae, Agelenidae) [Etude biométrique de la croissance des filières dans le développement post-embryonnaire de l'araignée *Agelena labyrinthica* (Clerck) (Araneae, Agelenidae)]. *Studia Societatis Scientiarum Torunensis, Sectio E (Zoologia)* 8: 253–334.
- Kovoor J (1977) La soie et les glandes séricigènes des arachnides. *L'Année Biologique* 16: 97–171.
- Kovoor J (1987) Comparative structure and histochemistry of silk-producing organs in arachnids. In: Nentwig W (Ed) *Ecophysiology of Spiders*. Springer-Verlag, Berlin, 160–186. [https://doi.org/10.1007/978-3-642-71552-5\\_12](https://doi.org/10.1007/978-3-642-71552-5_12)
- Kůrka A, Řezáč M, Macek R, Dolanský J (2015) Pavouci České republiky. Nakladatelství Academia, Praha, 623 pp.
- Michalik P, Ramírez MJ (2014) Evolutionary morphology of the male reproductive system, spermatozoa and seminal fluid of spiders (Araneae, Arachnida) — Current knowledge and future directions. *Arthropod Structure & Development* 43: 291–322. <https://doi.org/10.1016/j.asd.2014.05.005>
- Mikulska I (1969) Variability of the number of external spinning structures in female spiders *Clubiona phragmitis* C.L. Koch in populations to various degrees isolated. *Zoologica Poloniae* 19: 279–291.
- Mikulska I, Wiśniewski H (1979) Variation in the number of external spinning structures in the females of *Cyphepeira patagiata* (Clerck) (Araneae, Argiopidae) in population of Peninsula Hel. *Zoologica Poloniae* 27: 179–186.
- Mittmann B, Wolff C (2012) Embryonic development and staging of the cobweb spider *Parasteatoda tepidariorum* C.L. Koch, 1841 (syn.: *Achaeareana tepidariorum*; Araneomorphae; Theridiidae). *Development Genes and Evolution* 222: 189–216. <https://doi.org/10.1007/s00427-012-0401-0>
- Müller MC, Westheide W (1993) Comparative morphology of the sexually dimorphic orb-weaving spider *Argiope bruennichi* (Araneae: Araneidae). *Memoirs of the Queensland Museum* 33: 615–620. <http://biodiversitylibrary.org/page/40476084>
- Murphy JA, Roberts MJ (2015) *Spider Families of the World and Their Spinnerets, Part I: Text*. British Arachnological Society, York, 189 pp.
- Pekár S, Coddington JA, Blackledge TA (2012) Evolution of stenophagy in spiders (Araneae): evidence based on the comparative analysis of spider diets. *Evolution* 66: 776–806. <https://doi.org/10.1111/j.1558-5646.2011.01471.x>
- Platnick NI, Coddington JA, Forster RR, Griswold CE (1991) Spinneret morphology and the phylogeny of haplogyne spiders (Araneae, Araneomorphae). *American Museum Novitates* 3016: 1–73. <http://hdl.handle.net/2246/5043>
- Platnick NI, Shadab MU (1993) A review of the pirate spiders (Araneae, Mimetidae) of Chile. *American Museum Novitates* 3074: 1–30. <http://hdl.handle.net/2246/4971>
- Ramírez MJ (2014) The morphology and phylogeny of dionychan spiders (Araneae: Araneomorphae). *Bulletin of the American Museum of Natural History* 390: 1–374. <https://doi.org/10.1206/821.1>
- Richter CJJ (1970) Morphology and function of the spinning apparatus of the wolf spider *Pardosa amentata* (Cl.) (Araneae, Lycosidae). *Zeitschrift für Morphologie der Tiere* 68: 37–68. <https://doi.org/10.1007/BF00277422>
- Scharff N, Coddington JA (1997) A phylogenetic analysis of the orb-weaving spider family Araneidae (Arachnida, Araneae). *Zoological Journal of the Linnean Society* 120: 355–434. <https://doi.org/10.1111/j.1096-3642.1997.tb01281.x>
- Schütt K (2000) The limits of the Araneoidea (Arachnida: Araneae). *Australian Journal of Zoology* 48: 135–153. <https://doi.org/10.1071/ZO99050>
- Schütt K (2003) Phylogeny of Symphytognathidae s.l. (Araneae, Araneoidea). *Zoologica Scripta* 32: 129–151. <https://doi.org/10.1046/j.1463-6409.2003.00103.x>
- Shear WA (1981) Structure of the male palpal organ in *Mimetus*, *Ero*, and *Gelanor* (Araneoidea, Mimetidae). *Bulletin of the American Museum of Natural History* 170: 257–262. <http://hdl.handle.net/2246/1057>
- Shear WA, Palmer JM, Coddington JA, Bonamo PM (1989) A Devonian spinneret: early evidence of spiders and silk use. *Science* 246: 479–481. <https://doi.org/10.1126/science.246.4929.479>

- Thaler K, van Harten A, Knoflach B (2004) Pirate spiders of the genus *Ero* C.L. Koch from southern Europe, Yemen, and Ivory Coast, with two new species (Arachnida, Araneae, Mimetidae). *Denisia* 13: 359–368. [http://www.zobodat.at/pdf/DENISIA\\_0013\\_0359-0368.pdf](http://www.zobodat.at/pdf/DENISIA_0013_0359-0368.pdf)
- Tillinghast EK, Townley MA (1994) Silk glands of araneid spiders: selected morphological and physiological aspects. In: Kaplan D, Adams WW, Farmer B, Viney C (Eds) *Silk Polymers: Materials Science and Biotechnology* (ACS Symposium Series 544). American Chemical Society, Washington, DC, 29–44. <https://doi.org/10.1021/bk-1994-0544.ch003>
- Townley MA (1993) Silk use during proecdysis in the spider *Araneus cavaticus* (Araneae, Araneidae). PhD dissertation, Durham, New Hampshire, USA: University of New Hampshire.
- Townley MA, Horner NV, Cherim NA, Tugmon CR, Tillinghast EK (1991) Selected aspects of spinning apparatus development in *Araneus cavaticus* (Araneae, Araneidae). *Journal of Morphology* 208: 175–191 & C5–C7. <https://doi.org/10.1002/jmor.1052080204>
- Townley MA, Tillinghast EK, Cherim NA (1993) Molt-related changes in ampullate silk gland morphology and usage in the araneid spider *Araneus cavaticus*. *Philosophical Transactions of the Royal Society of London, Series B* 340: 25–38. <https://doi.org/10.1098/rstb.1993.0046>
- Townley MA, Tillinghast EK (2003) On the use of ampullate gland silks by wolf spiders (Araneae, Lycosidae) for attaching the egg sac to the spinnerets and a proposal for defining nubbins and tartipores. *Journal of Arachnology* 31: 209–245. [https://doi.org/10.1636/0161-8202\(2003\)031\[0209:OTUOAG\]2.0.CO;2](https://doi.org/10.1636/0161-8202(2003)031[0209:OTUOAG]2.0.CO;2)
- Townley MA, Tillinghast EK (2009) Developmental changes in spider spinning fields: a comparison between *Mimetes* and *Araneus* (Araneae: Mimetidae, Araneidae). *Biological Journal of the Linnean Society* 98: 343–383. <https://doi.org/10.1111/j.1095-8312.2009.01297.x>
- Townley MA, Harms D, Benjamin SP (2013) Phylogenetic affinities of *Phobetus* to other pirate spider genera (Araneae: Mimetidae) as indicated by spinning field morphology. *Arthropod Structure & Development* 42: 407–423. <https://doi.org/10.1016/j.asd.2013.04.003>
- Wąsowska S (1973) The variability of the number of external spinning structures within one population of *Araneus sclopetarius* Clerck. *Zoologica Poloniae* 23: 109–118.
- Wheeler WC, Coddington JA, Crowley LM, Dimitrov D, Goloboff PA, Griswold CE, Hormiga G, Prendini L, Ramírez MJ, Sierwald P, Almeida-Silva L, Alvarez-Padilla F, Arnedo MA, Benavides Silva LR, Benjamin SP, Bond JE, Grismado CJ, Hasan E, Hedin M, Izquierdo MA, Labarque FM, Ledford J, Lopardo L, Maddison WP, Miller JA, Piacentini LN, Platnick NI, Polotow D, Silva-Dávila D, Scharff N, Szűts T, Ubick D, Vink CJ, Wood HM, Zhang J (2016) The spider tree of life: phylogeny of Araneae based on target-gene analyses from an extensive taxon sampling. *Cladistics* <https://doi.org/10.1111/cla.12182>
- Wolff C, Hilbrant M (2011) The embryonic development of the Central American wandering spider *Cupiennius salei*. *Frontiers in Zoology* 8: 15. <https://doi.org/10.1186/1742-9994-8-15>
- World Spider Catalog (2017) Natural History Museum Bern. <http://wsc.nmbe.ch>, version 18.0. [accessed on 30 August 2017]
- Yoshida M (1999) Spinnerets silk spigots morphology of Araneidae, Tetragnathidae, Theridiidae and Linyphiidae (Araneae: Araneoidea). *Acta Arachnologica* 48: 1–22. <https://doi.org/10.2476/asjaa.48.1>
- Yu L, Coddington JA (1990) Ontogenetic changes in the spinning fields of *Nuctenea cornuta* and *Neoscona theisi* (Araneae, Araneidae). *Journal of Arachnology* 18: 331–345. <http://www.jstor.org/stable/3705439>

### Supplementary material 1

#### Material Examined

Authors: Mark A. Townley, Danilo Harms

Data type: specimens data

Copyright notice: This dataset is made available under the Open Database License (<http://opendatacommons.org/licenses/odbl/1.0/>). The Open Database License (ODbL) is a license agreement intended to allow users to freely share, modify, and use this Dataset while maintaining this same freedom for others, provided that the original source and author(s) are credited. Link: <https://doi.org/10.3897/evolsyst.1.14765.suppl1>